

Environmental implications of phosphate-based amendments in heavy metal contaminated alluvial soil

By

John S. Weber

U.S. Fish & Wildlife Service

Keith W. Goyne

University of Missouri

Todd Luxton

U.S. Environmental Protection Agency

Allen Thompson

University of Missouri

John Yang

Lincoln University

Administrative Report

U.S. Department of the Interior

U.S. Fish & Wildlife Service

U.S. Department of the Interior
Sally Jewell, Secretary

U.S. Fish & Wildlife Service
Dan Ashe, Director

U.S. Fish & Wildlife Service, Columbia, MO 2014

Any use of trade, product, or firm names is for descriptive purposes only and does not imply endorsement by the U.S. Government

TABLE OF CONTENTS

ABSTRACT.....	1
INTRODUCTION	2
MATERIALS AND METHODS.....	5
RESULTS AND DISCUSSION.....	19
CONCLUSIONS.....	42
REFERENCES	47
APPENDICES	53
A. SOIL PHOSPHORUS DOSING CALCULATIONS AND X-RAY FLUORESCENCE RESULTS.....	54
B. RAINFALL SIMULATION CALIBRATION DATA	56
C. CONCENTRATION OF METALS IN GRASS TISSUE AT ONE AND SIX MONTHS FOLLOWING VEGETATION WITH TALL FESCUE	62
D. SOIL AND WATER CHEMISTRY RESULTS FROM AMENDED AND UN- AMENDED SOILS	65
E. ADDITIONAL SPECTRA FROM X-RAY ABSORPTION NEAR EDGE SPECTROSCOPY ANALYSIS	73

LIST OF FIGURES

Figure	Page
1. The Big River of southeast Missouri (USA) with experimental soil sampling location at Washington State Park indicated.	6
2. Design schematic of the rainfall simulator.	12
3. Water chemistry data from the first rainfall simulation including (a) total phosphorus and dissolved orthophosphate, (b) total metals, and (c) dissolved metals.....	22
4. Water chemistry data from the second rainfall simulation including (a) total phosphorus and dissolved orthophosphate, (b) total metals, and (c) dissolved metals.....	26
5. Mass of P and Pb lost during RFS1 compared to RFS2 in kilograms per hectare.	28
6. Arithmetic mean of elemental composition of above ground grass tissue six months after vegetation with tall fescue including (a) lead in grass tissue, (b) cadmium in grass tissue, and (c) zinc in grass tissue	30
7. First derivative x-ray absorption near edge spectroscopy (XANES) spectra of untreated soils and select treated soils	32
8 First derivative of normalized X-ray absorption near edge spectroscopy (XANES) spectra of reference samples employed as model components for linear combination fitting	33
9. Relative abundance of Pb species determined by an linear combination fitting model fitted to the x-ray absorption near edge spectroscopy spectra at (a) first rainfall simulation, (b) in eroded material collected from effluents of first rainfall simulation, and (c) following second rainfall simulation.....	35
C.1. Arithmetic mean of cadmium concentrations of above ground grass tissue one and six months after vegetation with tall fescue (<i>Festuca arundinacea</i>).....	62
C.2. Arithmetic mean of lead concentrations of above ground grass tissue one and six months after vegetation with tall fescue (<i>Festuca arundinacea</i>).....	63
C.3. Arithmetic mean of zinc concentrations of above ground grass tissue one and six months after vegetation with tall fescue (<i>Festuca arundinacea</i>).....	64
E.1. Normalized and first derivative of normalized x-ray absorption near edge spectroscopy (XANES) spectra of reference samples employed as model components for linear combination fitting	73
E.2. Normalized and first derivative of normalized x-ray absorption near edge spectroscopy (XANES) spectra of untreated soils and select treated soils	74

LIST OF TABLES

Table	Page
1. Selected properties of untreated bulk stockpile, data represents the mean of 10 samples.....	7
2. Final plant available phosphorus concentrations in experimental soils determined using the Mehlich 3 procedure.	21
3. Mass of phosphorus and metals lost from rainfall simulation	24
4 Linear combination fitting results for x-ray absorption near edge spectroscopy analysis of control and amended soil samples after rainfall simulation	36
A.1. Washington State Park soil x-ray fluorescence analysis results	55
B.1. Rainfall simulation calibration data and calculations.....	56
D.1. Soil pH in water and in 0.01M CaCl ₂ at listed days after first P treatment.....	65
D.2. Arithmetic mean results of water chemistry analytes from the first (un-vegetated) rainfall simulation.....	66
D.3. Arithmetic mean results of water chemistry analytes from the second (vegetated) rainfall simulation.....	67
D.4. Water, sediment, and mass lost results from the first and second rainfall simulation events	68
D.5. Effect of rainfall simulation and treatment class on phosphorus loss from test beds.	69
D.6. Effect of rainfall simulation and treatment class on total cadmium loss from test beds.....	70
D.7. Effect of rainfall simulation and treatment class on total lead loss from test beds.	71
D.8. Effect of rainfall simulation and treatment class on total zinc loss from test beds.	72

Abstract

A diverse suite of research has focused on the immobilization of soluble Pb compounds in soil through the *in situ* application of phosphate-based amendments that induce formation of pyromorphites [Pb₅(PO₄)₃OH,Cl,F]. However, water quality threats associated with the P remediation technology are a concern, particularly when the strategy is considered for use in riparian areas. This study investigated the effects of P fertilizer application rates on metals and P loss via surface water runoff at different time intervals following P application to a lead contaminated alluvial soil. Accumulation of metals in the grass planted on the treatments was examined and speciation of the Pb compounds present before and after the treatments was investigated with X-ray absorption near edge spectroscopy (XANES). Soil collected from a contaminated floodplain was treated with Triple Super Phosphate (TSP) fertilizer at differing molar ratios of P to Pb: 0:1 (control); 4:1; 8:1; and 16:1. Following a six month reaction period, rainfall simulation (RFS) studies were initiated. Effluents from treated soils were collected during RFS events conducted at six months and one year post-treatment and analyzed to quantify total and dissolved P and Pb loss. At elevated P treatment levels (8:1, 16:1 P:Pb), P and total Pb concentrations in runoff were significantly greater ($p < 0.05$) than the control during the first round of rainfall simulation when the treatment units were un-vegetated. After one year of reaction time and the establishment of tall fescue (*Festuca arundinacea*) on the treatment units, total P content in effluents captured during the second RFS decreased by an order of magnitude and total Pb concentrations decreased by two to three orders of magnitude. Phosphorus concentration in runoff from 16:1 P:Pb treatment was significantly greater than all other treatments; however, total Pb concentrations were comparable amongst the treatments. Analysis of metal uptake into the tissues of tall fescue revealed a significant reduction in Pb uptake that

was most pronounced for the 16:1 P:Pb treatment. Statistical analysis with linear combination fitting (LCF) applied to XANES data of soil samples indicated that pyromorphite concentration ranged from 0% (control soil) to 32% (16:1 P:Pb, 1 year post-treatment) of the total Pb concentration. The addition of TSP stimulated pyromorphite formation but the amount of pyromorphite formed was comparable amongst the P-treatments. The findings of this study suggest that P application required to achieve a 4:1 P:Pb molar ratio may be a viable means of reducing Pb bioavailability in contaminated alluvial soils while minimizing concerns related to P loss from soils treated with this restoration strategy.

Introduction

Lead (Pb) has been mined for millennia and used by humans for an astoundingly wide variety of purposes. Consequently, Pb is one of the most common environmental pollutants worldwide (CDC, 2012; Eisler, 1988). The southern half of Missouri is home to several world class mining districts including the Southeast Missouri lead mining district, home to the world's largest known deposit of galena (PbS) (Seeger, 2008). As a consequence of the long term exploitation of the southeast Missouri galena deposits, contamination of soils and sediments in the area are widespread and may be toxic to the human and natural communities which inhabit the region (USEPA, 2007). Recently, it has been discovered that the vast majority of the alluvial soils of the Big River of St. Francois, Jefferson, and Washington Counties are contaminated with Pb above thresholds of concern for human health and the environment (Pavlowsky, 2010).

Remediation of Pb contaminated areas by traditional means of soil excavation, disposal, and replacement can be extremely expensive to complete on a large scale (USEPA, 1993).

In situ remedial technologies have been shown to be less invasive, reducing undesirable conditions such as fugitive dust emissions and heavy equipment exhausts, as well as overall

disruption of the landscape (Ma et al., 1993; 1995; Xu and Schwartz, 1994). Additionally, the volume and Pb concentrations present in the alluvial soils of the Big River make excavation and disposal technically impractical (Pavlowsky, 2010).

A number of previous studies have successfully altered soil Pb chemistry through the addition of inorganic phosphate compounds that convert soil Pb species to less soluble pyromorphite minerals [Pb₅(PO₄)₃(OH, Cl, F)]. Pyromorphites are the most thermodynamically stable and insoluble Pb minerals over a large pH range (Nriagu, 1974). The stability of pyromorphites under a wide variety of environmental conditions makes Pb immobilization by phosphorous amendments an effective technique, as accidental pyromorphite ingestion will not yield bioavailable lead (Zhang et al. 1998; Arnich et al. 2003). The creation of pyromorphites and commensurate reductions in bioavailability of Pb contaminated soils has been well documented (Ma et al., 1993; 1995; Xu and Schwartz, 1994; Ruby et al., 1994; Laperche et al., 1996; Zhang et al., 1998).

However, the addition of large quantities of P to soils is an environmental concern, as P loss to aquatic ecosystems is associated with eutrophication (Theis and McCabe, 1978; Sharpley and Halvorson, 1994; Sims, 1993; Dermatas et al., 2008). Potential issues of P leaching from Pb contaminated soils treated with P amendments have only been lightly discussed or mentioned by studies investigating the feasibility of P treatment (Basta and McGowen, 2004; Cao et al., 2002; Chen et al., 2006; Dermatas et al., 2008; Tang et al., 2004; Yang and Tang, 2007). The leaching of substantial quantities of P from treated soils has been demonstrated in acidic and alkaline soils under a variety of laboratory conditions (Dermatas et al., 2008; Kilgour et al., 2008; Stanforth and Qui, 2001). However, there exists a paucity of research contemplating the consequences of P treatment under conditions likely to occur in the environment (Dermatas et al., 2008).

Consequently, this study focuses on elucidating P loss from contaminated soils amended with inorganic P fertilizer in a simulated environment, a necessary step for evaluating potential eutrophication of aquatic ecosystems neighboring P remediated soils.

In addition to considering the fate and transport of P following treatment of Pb contaminated soils, it is of utmost importance to confirm the formation of pyromorphites as an indicator of reductions in the bioavailability of Pb species present in the soil (Scheckel et al., 2003). A wide variety of techniques have been employed to confirm pyromorphite formation including selective sequential extraction (SSE) procedures, *in vitro* physiologically-based extraction tests (PBET), energy dispersive x-ray spectroscopy (EDX), and scanning electron microscopy (SEM) (Ryan et al., 2001; Cao et al., 2003; Scheckel et al., 2003; 2005; Davis et al., 1993; Yang et al., 2001). However, SSE and the PBET tests have been shown to artificially create pyromorphites during the digestion phase of the analyses (Scheckel et al., 2003; 2005), and visual confirmation of pyromorphites using SEM and EDX has been shown to be of limited utility due to the similarity of hexagonal pyromorphite crystals to a variety of other crystalline soil components (Scheckel and Ryan, 2003). Consequently, scientists have turned to advanced synchrotron spectroscopic techniques to confirm pyromorphite formation in an exacting and non-destructive manner (Cotter-Howells et al., 1994; Ryan et al., 2001; Scheckel and Ryan, 2002; Scheckel and Ryan, 2003; Scheckel and Ryan, 2004). X-ray absorption spectroscopy (XAS) in combination with advanced statistical models is frequently used to identify different metals species in soil environments and XAS is particularly useful when studying Pb contaminated soils amended with P (Isaure et al., 2002; Roberts et al., 2002; Scheinost et al., 2002; Scheckel and Ryan, 2004). Consequently, the current study employed XAS as a reliable means of confirming and estimating pyromorphite formation.

The objectives of this study were to: (1) determine the relationship between concentrations of P and metals eluviated from three treatment classes of P-treated, Pb-contaminated soils during simulated rainfall events conducted using un-vegetated soil at six months post-treatment and a vegetated soils at twelve months post-treatment; (2) confirm potential reductions in Pb bioavailability within the treated soils by measuring the metal content of tissues from grasses grown on the treatment units; and (3) investigate pyromorphite formation in the P-treated soils as a function of P application.

Materials and Methods

Soil collection

Kaintuck fine sandy loam soil (coarse-loamy, siliceous, superactive, nonacid mesic Typic Udifluvents) was collected from the Big River floodplain at Washington State Park, near DeSoto, Missouri, USA (38° 5'13 N, 90°40'28 W) (Fig.1).

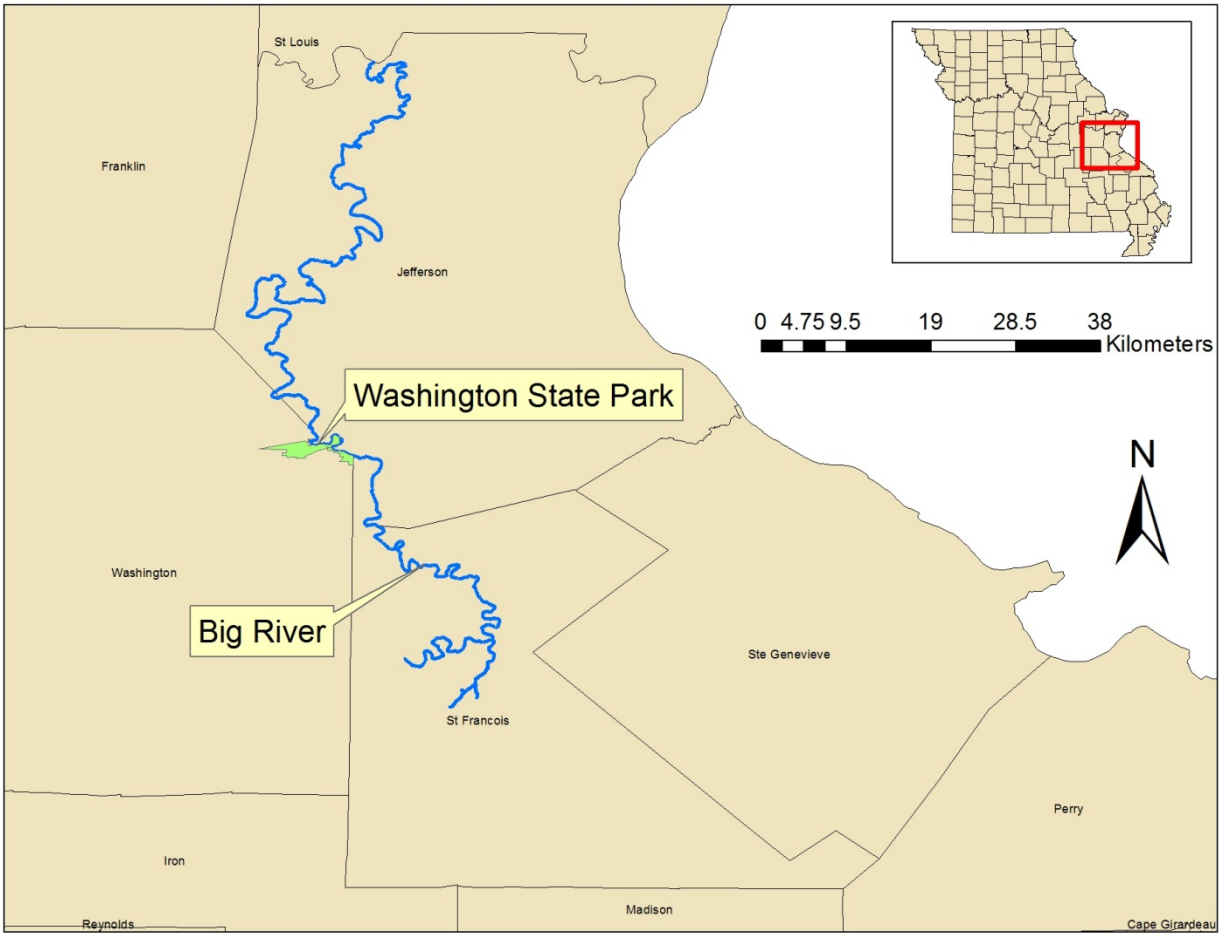


Figure 1. The Big River of southeast Missouri (USA) with experimental soil sampling location at Washington State Park indicated.

Table 1. Selected properties of untreated bulk stockpile, data represents the mean of 10 samples.

Soil Property	Result
USDA Classification	Typic Udifluent
Textural Class	Silt loam
Bulk Density, g/cm ³	1.2 (±0.0) †
Cation Exchange Capacity, cmol kg ⁻¹	22.5 (±0.2)
Cation Exchange Capacity NH ₄ Cl, cmol kg ⁻¹	16.0 (±0.1)
Percent Base Saturation	92.4 ((±0.5)
pH water	7.3(±0.0)
pH salt (.01 M CaCl ₂)	7.6 (±0.0)
BaCl ₂ Extractable Acidity, cmol kg ⁻¹	1.7 (±0.1)
Total organic carbon, g kg ⁻¹	21.0 (±0.0)
Total Nitrogen, g kg ⁻¹	2.0 (±0.1)
Mehlich 3 extractable elements, mg kg ⁻¹	
Al	528 (±3.8)
Ca	2572 (±10.7)
Cu	25 (±0.1)
Fe	263(±1.4)
K	53 (±0.1)
Mg	611 (±1.7)
Mn	100 (±0.9)
Na	60 (±2.0)
P	32 (±1,4)
Zn	226 (±0.6)
Total Elemental Concentration mg kg ⁻¹	
As	7 (±0.1)
Ba	940 (±11.1)
Cd	10 (±0.4)
Cu	72 (±0.3)
Pb	2192 (±12.7)
Mn	1978 (±15.1)
Zn	634 (±4.3)

† Error in parentheses represents the standard error.

Vegetative cover at the site was predominantly tall fescue (*Festuca arundinacea* Schreb; Kentucky 31). Site selection was guided by the use of a hand held X-ray fluorescence (XRF) spectrometer (Thermo Fisher, Waltham, MA) which was used to target surface soil concentrations of $>1500 \text{ mg kg}^{-1}$ Pb (Appendix A, Table A.1). After removal of the sod, samples were collected from several shallow, hand-dug pits to a depth of 15 cm. All soil was collected from within a 100 m^2 area to minimize differences in spatial variability between samples. Moist soils were passed through a 4 mm screen in the field to remove roots and coarse fragments. Soils from the pits were bulked and mechanically mixed to create a single stockpile of soil. Core samples (7.5 cm by 7.5 cm, diameter by height) used to quantify soil bulk density were collected within the sample area using an Uhland core sampler prior to sieving and mixing.

Initial soil sample characterization

After thorough air drying and mixing, the bulk soil stockpile was sieved to $< 2 \text{ mm}$ for use in all experimental trials. Sieving was accomplished by forcing air-dried soil over frames mounted with 2 mm hardware cloth. Ten composite samples comprised of five aliquots each were collected from the bulk stockpile for determination of general soil properties prior to P-treatment. Analyses including pH_{water} , pH_{salt} (0.02M CaCl_2), particle size distribution, extractable Al, titratable acidity, buffered and unbuffered cation exchange capacity (CEC), organic carbon, Mehlich 3 P and total N content were determined by the University of Missouri's Soil Characterization Laboratory following procedures recommended by the United States Department of Agriculture, Natural Resource Conservation Service (USDA, 2004). Total elemental analysis of As, Ba, Cd, Co, Cr, Cu, Mn, Ni, Pb, Zn using the HNO_3 -microwave digestion procedure (USEPA method 6010B (USEPA, 2012) was performed by the Missouri

Department of Natural Resources' State Environmental Laboratory, Jefferson City, MO (Table 1).

Phosphate treatment of soils

Soil was amended with Triple Super Phosphate [TSP; $\text{Ca}(\text{H}_2\text{PO}_4)_2$] at one of four molar ratios of P to Pb (P:Pb): 0:1 (control); 4:1; 8:1; and 16:1 (dosing calculations are available in Appendix A). Four replicates of each treatment level were created by placing 108 kg of air-dried soil (1.5% moisture by mass) from the bulk stockpile into commercially available 70 gallon polyethylene tanks. The soils were then treated with a granulated form of TSP acquired from a local commercial source (Bonide Products, Inc., Oriskany, NY). The TSP application was administered as an equivalently split application on two separate dates. The initial application was used to induce acidification and, forty days later, the second application was applied to achieve the desired P:Pb molar ratios for each treatment (Melamed et al., 2002). On each application date, one-quarter of the total TSP mass required to achieve the desired molar ratio was added to the soil, thoroughly mixed by hand and mechanical mixer, and then the process was repeated (Yang et al., 2001). Treated soils were then moistened with deionized water until approximate field capacity was achieved, and the treated soils were allowed to react for 60 days (deionized water was periodically added to maintain field capacity throughout the reaction period). Following the first reaction period, hydrated lime ($\text{Ca}(\text{OH})_2$) was added to the treatments to achieve a soil pH 6.5-7.5, thereby simulating normal agronomic conditions and enhancing pyromorphite formation (Chappell and Scheckel, 2007). The control treatment was not limed, as native pH_{water} was approximately 7.8 (Table 1). Following liming, all treatment soils were kept moist for 90 days in a greenhouse at approximately 25° C. Values for soil pH_{water} and pH_{salt} measured over time can be found in Appendix D.

Rainfall simulation test beds

Sixteen RFS test beds were fabricated using 16 gauge sheet steel to the following dimensions: 50 cm x 30 cm x 25 cm (length x width x depth). An adjustable V-notch front was attached to the front of the RFS test beds to channel surface runoff to a collection point. Perforated 0.5 inch (OD) Schedule 40 PVC pipe was used to construct a subsurface drainage collection point with 2 ports located on the exterior of the drainage box below the V-notch. Silicone caulk was used to hold the PVC tubing in place and prevent leaking at the ports. All surfaces of the RFS boxes were painted using a lead-free latex paint. Following construction of the RFS test beds, all of the beds were cleaned with a dilute HNO₃ (1% by volume) and rinsed in triplicate with deionized water.

The RFS beds were then filled with screened and washed medium grade (.08-.3 mm) sand (Quikrete, Atlanta, GA) to a depth of 10 cm, completely covering the PVC drainage tubing. Next a sheet of landscape fabric cut to the inside dimension of the box was used to cover the sand to prevent intrusion of the treatment soil into the underlying substrate. Soil associated with each of the four P:Pb treatment levels was placed into individual test beds to a depth of approximately 10 cm, and compacted with a steel tamper to a bulk density of 1.2 g cm⁻³ (the bulk density measured from field samples; Table 1). A total of 16 test beds were prepared and each treatment level was replicated in quadruplicate.

First rainfall simulation

Rainfall simulation studies were completed using the rainfall simulation tower at the University of Missouri, described in Regmi and Thompson (2000) (Fig. 2), using deionized, reverse osmosis (DIRO) water. Briefly, the 1x1 m laboratory scale simulator operates under a positive displacement principle to provide a mean droplet diameter of 2.6 mm. Pre-weighed and

acid washed calibration buckets were allowed to fill for 6 minutes in the rainfall simulator once the device reached equilibrium. After the rainfall simulator was calibrated and rainfall rates were verified, the experimental test beds were placed on a test stand (RFS calibration data are in Appendix B). The test stand was elevated to a slope of 2% for all tests. Soils were exposed to simulated rainfall for 1.5 hours at an average rate of 5 cm hr^{-1} . All effluents were collected from the V trough of the soil boxes under a shield designed to prevent simulated rainfall from directly entering the sampling container. All effluents were collected in a pre-weighed 1 gallon high density polyethylene bucket, approximately 20.3 cm in diameter.

Leachate was not observed emanating from drainage tubes within the sand substrate, eliminating the need to collect and analyze subsurface drainage waters. Following the 1.5 hour test period, bulk effluents and RFS test beds boxes were removed from the simulator. During all of the tests a small portion of soil was trapped in the trough but not collected in the bulk effluent sample. This small portion of soil was carefully irrigated into a 4 oz. I-CHEM glass jar using DIRO water for further analysis and filtration.

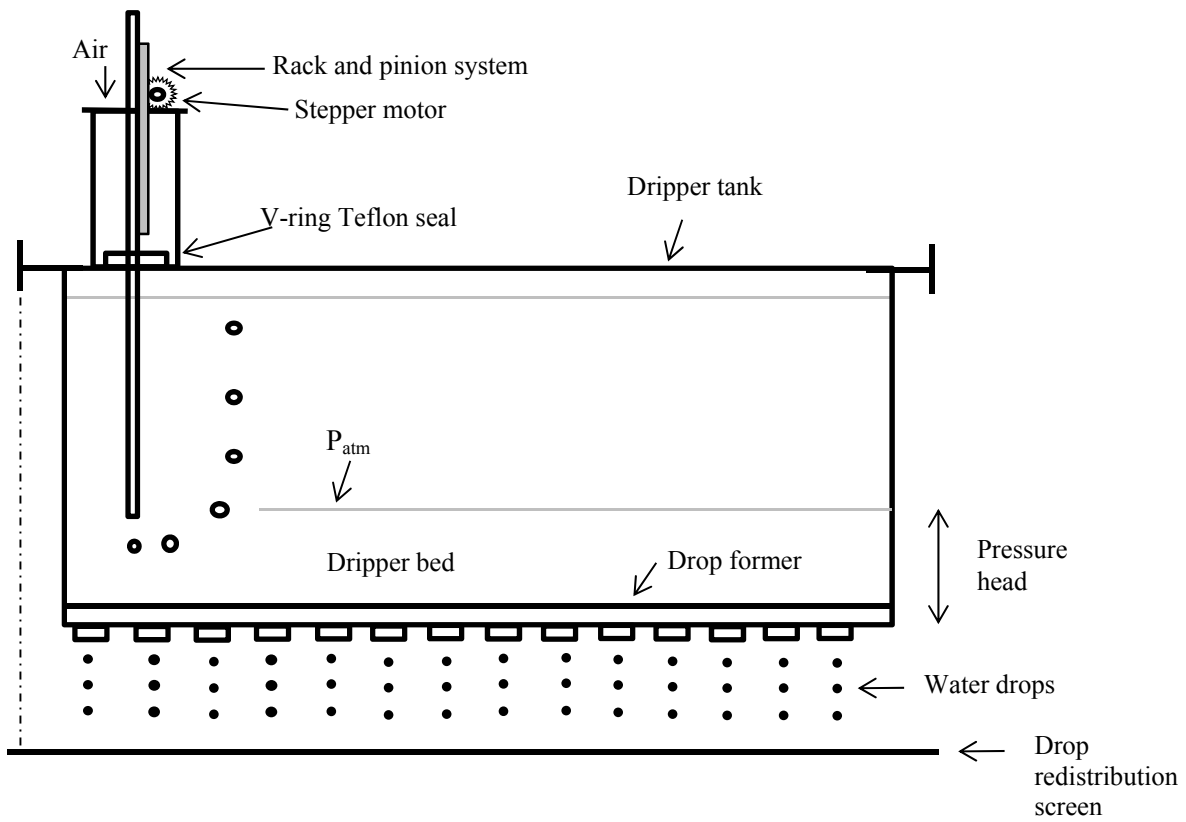


Figure 2. Design schematic of the rainfall simulator (after Regmi and Thompson, 2000).

Effluent water sample processing

Following RFS test period, the combined total mass of the water, eroded material and bucket was measured and recorded. The sample container was then placed on a stir plate and an acid washed stir bar was added to thoroughly distribute sediment throughout the solution; samples were stirred for 5 minutes at 1000 rpm. After mixing, aliquots for total metals and total P analyses were collected using a Geotech GeoPump (Denver, CO) peristaltic pump and new Masterflex (Vernon Hills, IL) Platinum Silicone L/S 15 tubing by submerging the tubing into a continuously stirred sample. Next, the bulk sample container was weighed and the mass was recorded again (Appendix D). Samples for dissolved metals and dissolved orthophosphate analysis were collected by attaching a Geotech Dispos-a-filter (Denver, CO), 0.45 μm high capacity in-line filter to the peristaltic pump and tubing. Samples for total and dissolved metals were immediately preserved using a 10% (v/v) HNO_3 solution (Ricca Chemical Company, Arlington, TX). Samples for total P were preserved using 1:1 H_2SO_4 sample preservation ampules (EaglePicher Scientific, Joplin, MO). Following collection of water samples, the bulk sample effluent and container were weighed a final time. All water samples were stored in 250 ml high density polyethylene containers, certified I-CHEM clean (Nalgene Corp., Waltham, MA), at 4°C in the dark.

Eroded soil processing

The remainder of the bulk effluent sample was filtered through pre-weighed, Fisher Scientific (Pittsburgh, PA) Q2 Fine Porosity Filter Paper (Particle retention 1-5 μm). Filter papers were placed in acid washed glass funnels and the bulk effluent and trough pellets were carefully poured through the filter paper. Remaining soil in the sample containers was rinsed

onto the filter paper using Barnstead (Asheville, NC) ultra-pure water until no visible soil particles were left in the sample containers. Following drainage of the water through the filter paper, soil plus filter papers were placed dried at 70°C for 48 hours, and mass of filter paper plus soil was measured (Appendix D). Eroded soil from the first RFS was analyzed for plant available P via the Mehlich 3 process by the Soil Characterization Laboratory.

Mass of total P and total metals lost to erosive flows was calculated (Table 3) according to the following equation:

$$\frac{C \text{ mg L}^{-1} * V \text{ L}}{A \text{ m}^2} = \text{Total mass lost (mg/m}^2\text{)}$$

where C = concentration of contaminant of concern in effluent (e.g. Total Pb)
and V = volume of runoff collected
and A = surface area of test bed .

Effluent water digestion and preparation

Non-filtered water samples collected for total metals and dissolved metals were digested by placing 5 ml of sample and 1 mL of HNO₃ into a 50 ml quartz reaction vessel and heating the sealed high pressure vessel assembly in a Perkin-Elmer Multiwave Digestion System according to specifications in a pre-programmed method. After cooling, digested samples were transferred to a storage container and diluted to a final volume of 50 ml (2% HNO₃ matrix). Total phosphorus was digested using the above described methodology and dilutions using sulfuric acid and the ammonium persulfate digestion procedure described in USEPA method 365.1 (USEPA, 2007b). The dissolved orthophosphate samples were directly analyzed without further

digestion or acidification. Sample digestion and analysis (see following section for details) were performed at the Missouri Department of Natural Resources' State Environmental Laboratory.

Water Chemistry Analysis

Total and dissolved metals content of digested water samples were quantified using a Perkin-Elmer Sciex Elan DRCe (Waltham, MA) inductively coupled plasma-mass spectrometer (ICP-MS) using the quantitative analysis mode. Internal standards were rhodium (Rh; 0.01 mg L⁻¹) and bismuth (Bi; 0.01 mg L⁻¹). Concentrations of standards used in the calibration curves were as follows: Cr, Co, Ni, As, Pb - 0.005, 0.01, 0.02, 0.04 mg L⁻¹; Zn – 0.075, 0.15, 0.3 mg L⁻¹; Ag – 0.0015, 0.003, 0.0066, 0.012 mg L⁻¹. When concentrations of any sample exceeded the highest calibration standard, the sample was diluted 10-fold using a Cetac ASD-500 autodiluter in a serial fashion, until the concentration fell within the confines of the standard curve. Masses monitored included: ⁵²Cr and ⁵³Cr; ⁵⁹Co; ⁶⁰Ni and ⁶²Ni; ⁶⁶Zn and ⁶⁸Zn; ⁷⁵As; ¹⁰⁷Ag and ¹⁰⁹Ag; ¹¹¹Cd and ¹¹⁴Cd; and ²⁰⁶Pb, ²⁰⁷Pb, ²⁰⁸Pb. Where multiple masses were monitored, masses were selected for reporting based on least interferences. Lead was reported as the sum of three masses (²⁰⁶Pb+²⁰⁷Pb+²⁰⁸Pb).

Digested water samples for total phosphorus and dissolved orthophosphate were analyzed colorimetrically using a Lachat QuikChem 8500 Series 2 FIA System (Loveland, CO) following USEPA method 365.1 (USEPA, 2007b). When concentrations of any sample exceeded the highest calibration standard, the sample was diluted 10-fold using a PDS200 dilutor system in a serial fashion, until concentrations fell within the confines of the standard curve.

Fescue establishment on test beds and Second Rainfall Simulation

Following the first RFS, the test beds were planted with tall fescue (*Festuca arundinacea* Schreb; Kentucky 31) to simulate average pasture conditions observed in the Big River floodplain of southeast Missouri, USA. The tall fescue was watered once a week with a volume of DIRO equal to one half of the soil volume in the test beds, or approximately 8 liters per test bed per week. Air temperature was kept constant at approximately 25°C. The tall fescue was allowed to grow for 90 days after the first RFS when all vegetation above the top lip of the test beds was removed. Tissue samples were then rinsed with DIRO for one minute to remove any soil particles from the surface of the leaves. Vegetative tissue samples were oven-dried at 70°C for 48 hours prior digestion by USEPA method 3052 *Microwave Assisted Digestion of Siliceous and Organically Based Matrices* (USEPA, 2012b) and total metals analysis by ICP-MS. Vegetative tissue samples were also collected, prepared and dried according to the same procedure described above 180 days after the first RFS and immediately prior to the second RFS. The ICP-MS analyses were conducted using the same procedures and instrumentation as described above.

In order to gauge the impact of time and vegetative cover on the erosion of soil and loss of associated contaminants from the test beds, a second RFS test was conducted 180 days after the first simulation. All of the experimental protocols described during the first RFS were utilized during the second RFS to facilitate comparison of results. At the conclusion of the second RFS, composite soil samples were collected and analyzed for available P (Mehlich 3 analyses) (Table 2.).

Statistical analyses for rainfall simulation and metals content of grass tissue

A one-way analysis of variance (ANOVA) was used to analyze the RFS data using the statistical analysis software SAS (SAS Inst., 1999). The Holm-Sidak method was used to evaluate differences between the means. Treatments included phosphate application rate (0:1, 4:1, 8:1, and 16:1 P:Pb) and vegetative cover with grass (grass cover and no grass cover). Statistical differences were tested at $\alpha = 0.05$.

X-ray absorption near-edge structure spectroscopy (XANES)

Pb LIII-edge (13 035 eV) X-ray absorption spectra were collected at the Materials Research Collaborative Access Team's (MRCAT) beamline 10-ID, Sector 10 at the Advanced Photon Source at the Argonne National Laboratory, Argonne, IL. The electron storage ring was operated in top-up mode at 7 GeV. Spectra were collected in transmission and fluorescence modes with either a Lytle or an element solid-state silicon drift detector at room temperature. The samples were prepared as thin pellets with a hand operated IR pellet press and the samples were secured to sample holders using Kapton tape. For each sample, a total of fifteen to seventeen scans were collected and averaged. Data were analyzed using the Athena software program (Ravel and Newville, 2005). The results for the samples were compared with those from synthesized minerals and mineral specimens acquired from the Smithsonian National Museum of Natural History (USA). All minerals were verified with XRD before use as reference materials for assessment of Pb solid-state speciation.

Soil Pb speciation was determined by comparison of Pb standards to the field samples by Linear Combination Fitting (LCF). Linear Combination Fitting refers to the process of selecting a multiple component fitting function with a least-squares algorithm that minimizes the sum of

the squares of residuals. A fit range of -20 to 50 eV was utilized for the X-ray absorption near-edge structure (XANES) portion of the XAS spectra and up to four variables. The best fitting scenarios are determined by the smallest residual error (χ^2) and the sum of all component fractions being close to 1. The reference samples ultimately selected for use in the LCF model were plumboferrite (PbFe_4O_7), plumbonacrite ($\text{Pb}_5\text{O}(\text{OH})_2(\text{CO}_3)_3$), chloropyromorphite ($\text{Pb}_5(\text{PO}_4)_3\text{Cl}$), Pb-sorbed to hydroxyapatite complex ($\text{Ca}_5\text{Pb}_5(\text{PO}_4)_6(\text{OH})_2$), galena (PbS), hydrocerussite ($\text{Pb}_3(\text{CO}_3)_2(\text{OH})_2$), anglesite (PbSO_4), plumbomagnetite (PbFe_2O_4), litharge (PbO), lead hydroxide ($\text{Pb}(\text{OH})_2$), and Pb sorbed to humic and fulvic acids, goethite, gibbsite, kaolinite, bentonite, and calcite. In general, LCF results are accurate to $\pm 5\%$, thus results less than 10% weight contribution should be interpreted with caution even though these components improve the overall error within the fitting process.

Results and Discussion

Effluent water chemistry results from un-vegetated test beds

The potential for negative impacts to surface water quality from P treatment of heavy metals contaminated soil was examined in this study by measuring the concentrations of P and heavy metals in effluents generated during RFS tests. To the best of our knowledge, this is the first reported experiment to use RFS to evaluate P and metals loss from heavy metal contaminated soils remediated via P application. Unlike batch and column leaching studies (Dermatas et al., 2008; and Kilgour et al., 2008), predominantly used to study P based Pb immobilization, RFS studies provide a more realistic scenario of determining whether mobilized contaminants could potentially enter surface water environments following P treatment of soils under normal precipitation scenarios.

Un-vegetated control and treated soils were exposed to RFS following a six month reaction period in an effort to capture water quality and soils data that could approximate field conditions for a P treated, Pb contaminated soil. As expected, total and dissolved phosphorus concentrations in effluent from the 16:1 P:Pb phosphorus treatment class were substantially elevated; total P concentration in effluent from the 16:1 P:Pb treatment was 36 times greater than the control soil (0:1 P:Pb) and nine times greater than the 4:1 P:Pb treatment class (Fig. 3). Due to the novelty of this work, direct comparisons of P concentrations to previous studies are not readily facilitated by the existing literature. However, concentrations of P released into solution during this study are similar to those observed during column leaching and batch reaction experiments conducted by Dermatas et al. (2008) (1 to 40 mg L⁻¹ P) and Kilgour et al. (2008) (up to 23 mg L⁻¹ P), although substantially less than P in column leachates reported by Yang et al. 2002 (>300 mg L⁻¹). Cao et al. (2002) suggest that up to 20% of the total P added (at P:Pb 4:1)

leached vertically from an *in situ* treatment area, but did not provide specific P effluent data. Another study with lower P dosing amounts compared to the majority of treatability studies presented in the literature reported up to 10% of total P was lost through column leaching (Basta and McGowen, 2004).

Table 2. Final plant available phosphorus concentrations in experimental soils determined using the Mehlich 3 procedure.

Treatment Class	Mehlich3 P (mg kg ⁻¹)
Control	30.53 ^a
4:1	480.9 ^b
8:1	947.1 ^c
16:1	2074 ^d

^{-a}: One way ANOVA used to determine differences between groups. Groups marked with the same letter are not significantly different from each other at $\alpha=.05$.

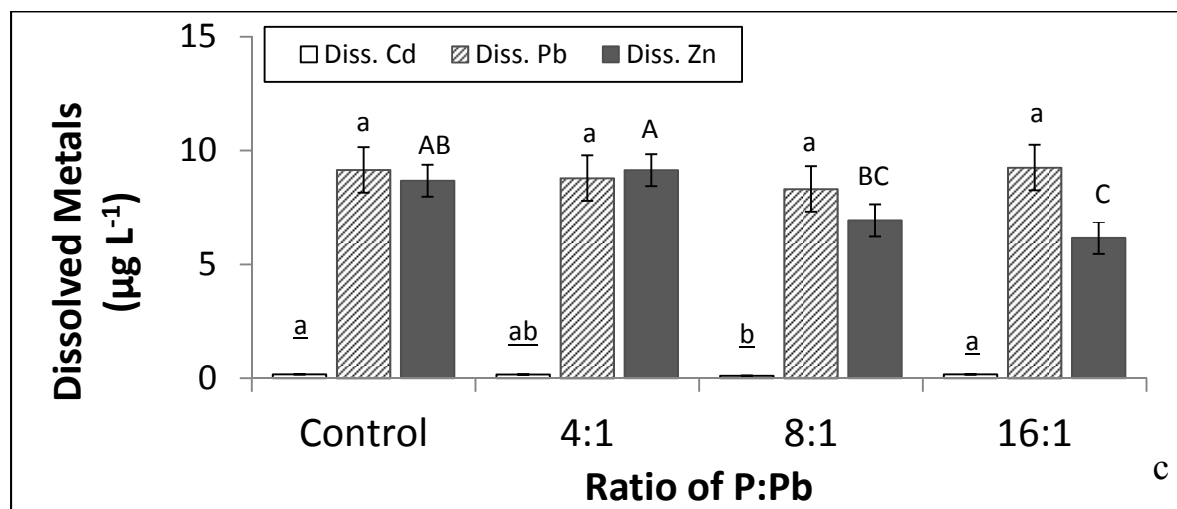
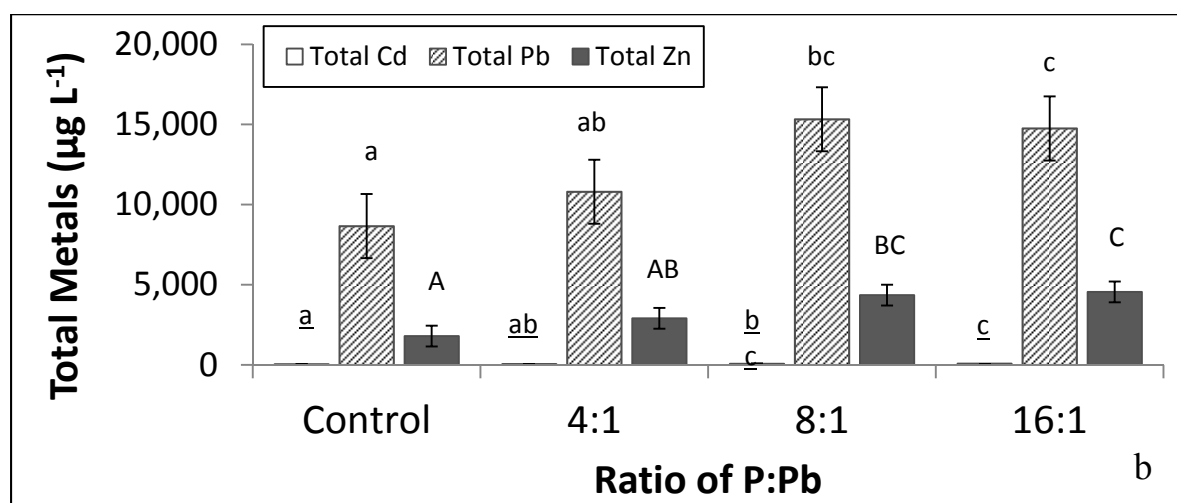
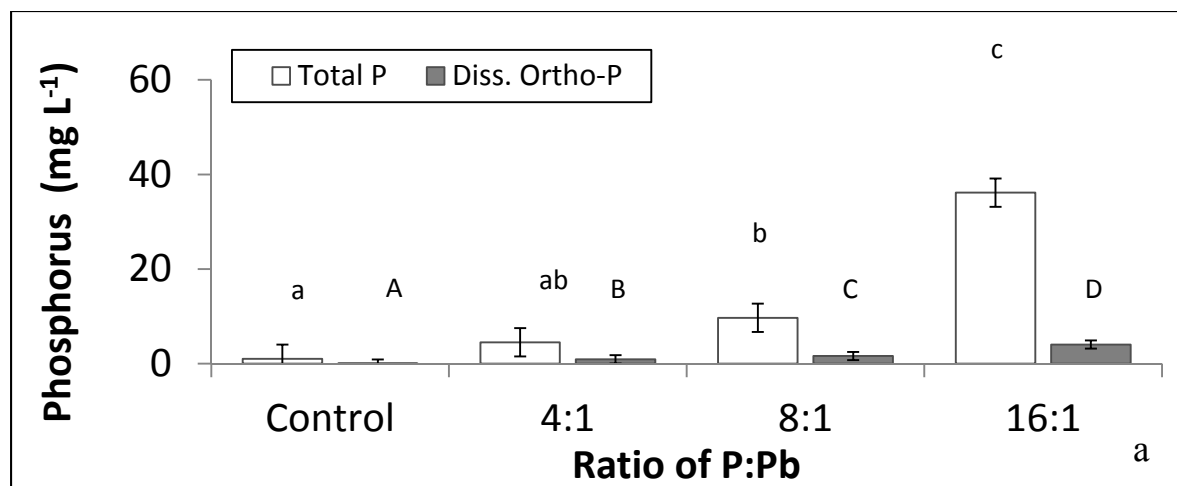


Figure 3. Water chemistry data from the first rainfall simulation including (a) total phosphorus and dissolved orthophosphate, (b) total metals, and (c) dissolved metals. Error bars represent standard error.

Significantly greater concentrations of total metals were observed in runoff effluents as a function of P treatment (Fig. 3), especially from the two elevated treatment levels (8:1 and 16:1 P:Pb). For example, total Pb concentration in the effluents from the 8:1 and 16:1 P:Pb treatments exceeded $14,500 \text{ mg L}^{-1}$, and total Pb concentrations in effluents from these treatments were significantly greater ($p < 0.05$) than the control soil ($< 8700 \text{ mg L}^{-1}$). Increased total metal concentrations in effluents with P treatment were consistent between Pb, Zn, and Cd (Fig. 3). It is possible that the elevated concentrations of total metals observed in the effluents of the first RFS is due to increased colloidal transport commensurate with disturbance introduced during our treatment regimen. Phosphorus treatment did not significantly affect the concentrations of dissolved Pb and minimally influenced dissolved Cd concentrations during the first RFS, but dissolved Zn concentration was noted to decrease significantly with increasing P application.

Because total volume of runoff effluents and mass of eroded materials were not significantly different between all of the treatments (Appendix D), we can safely state that P treatment is not having a physical effect on the treated soils. However, the overall mass of P and total metals lost (Table 3) increases significantly at the two highest treatment classes (8:1 and 16:1 P:Pb ratios). Total phosphorus lost at the 16:1 P:Pb ratio during un-vegetated RFS1 at 6.01 kg/ha was 33 times greater than values reported for un-amended soils which parallels trends reported for the effluent concentrations. These results are generally up to two orders of magnitude greater than results reported from other P transport studies utilizing RFS; and further, it is important to note that the final Mehlich 3 P concentrations reported here

Table 3. Mass of phosphorus and metals lost from rainfall simulation. Values represent the arithmetic mean of four repetitions per treatment level.

Rainfall Simulation and Treatment Class	P loss kg/ha	Cd loss kg/ha	Pb loss kg/ha	Zn loss kg/ha
RFS1- Control	0.18 ^{a,A}	0.01 ^{a,A}	1.54 ^{a,A}	0.32 ^{a,A}
RFS1-4:1	0.76 ^{a,b,A,B,C}	0.01 ^{a,A}	1.81 ^{a,b,A,B}	0.48 ^{a,A}
RFS1-8:1	1.75 ^{b,C}	0.01 ^{b,B}	2.76 ^{a,b,C}	0.78 ^{b,B}
RFS1-16:1	6.01 ^{c,D}	0.01 ^{b,B}	2.45 ^{b,B,C}	0.76 ^{b,B}
RFS2- Control	0.09 ^{a,A,B}	0.0001 ^{a,C}	0.004 ^{a,D}	0.01 ^{a,C}
RFS2-4:1	0.17 ^{b,A,B}	0.0001 ^{a,C}	0.004 ^{a,D}	0.01 ^{a,C}
RFS2-8:1	0.25 ^{c, A,B}	0.0001 ^{a,C}	0.007 ^{a,D}	0.01 ^{a,C}
RFS2:16:1	0.38 ^{d,A,B}	0.0002 ^{a,C}	0.005 ^{a,D}	0.01 ^{a,C}

^{-a}: One way ANOVA and the Holm-Sidak method used to determine differences between treatment groups. Groups marked with the same lower case letter are not significantly different from each other within the RFS at $\alpha=0.05$.

^{-A}: One way ANOVA and the Holm-Sidak method used to determine differences between RFS events. Groups marked with the same upper case letter are not significantly different from each other between the RFS at $\alpha=0.05$.

(Table 2) are also an order of magnitude greater than most agronomic studies (Blanco-Canqui et al., 2004; Sharpley and Kleinman, 2003; Schroeder et al., 2004) involving inorganic and organic P sources. Differences in P loss among these studies and the current are likely attributable to methods used for the incorporation and mixing of added P and the quantities of P applied.

Effluent water chemistry results from vegetated plots from the second rainfall simulation

After six months of additional aging and coverage of the RFS test beds with a sod-forming turf grass, a second RFS experiment was conducted on the same experimental soils. Concentrations of total and dissolved P, as well as total metals and dissolved Pb, dramatically decreased during the second RFS (Fig. 4). Total Pb, Zn, and Cd concentrations in runoff effluents were reduced two to three orders of magnitude and total phosphorus concentration was reduced by one order of magnitude when compared to results from the first RFS. Additionally, concentrations of dissolved Pb and P were reduced by nearly one-half. With respect to dissolved Pb, concentrations were not significantly different across treatments and controls during the second RFS. Notably, we observed large increases in the concentrations of dissolved Zn (3- to 4-fold) and dissolved Cd (2- fold) in the second RFS, as compared to the first RFS, although there were no significant differences in dissolved Zn and Cd amongst the four P application treatments during the RFS2. These observations suggest a baseline effect of dissolved metals eluviation from the soil that is not controlled by P treatment.

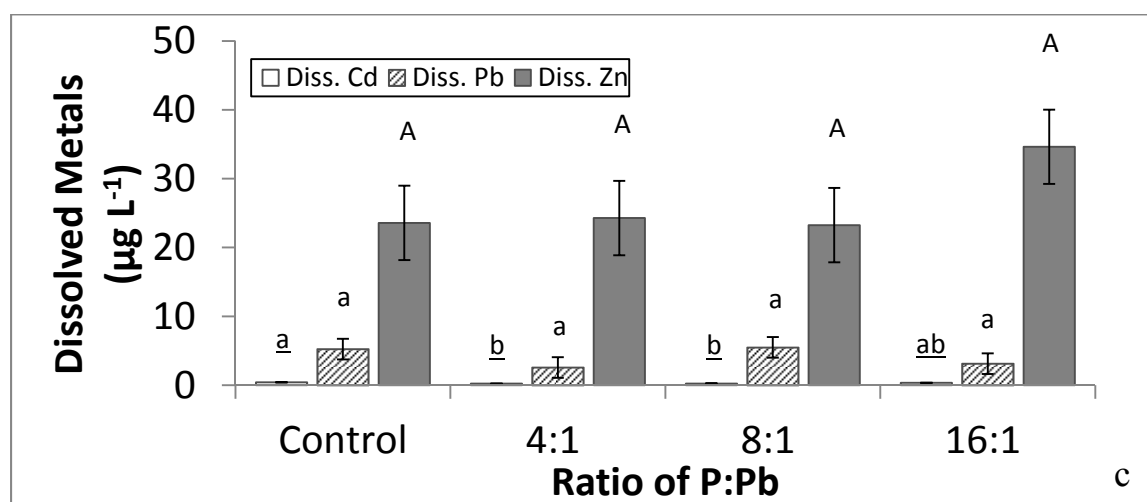
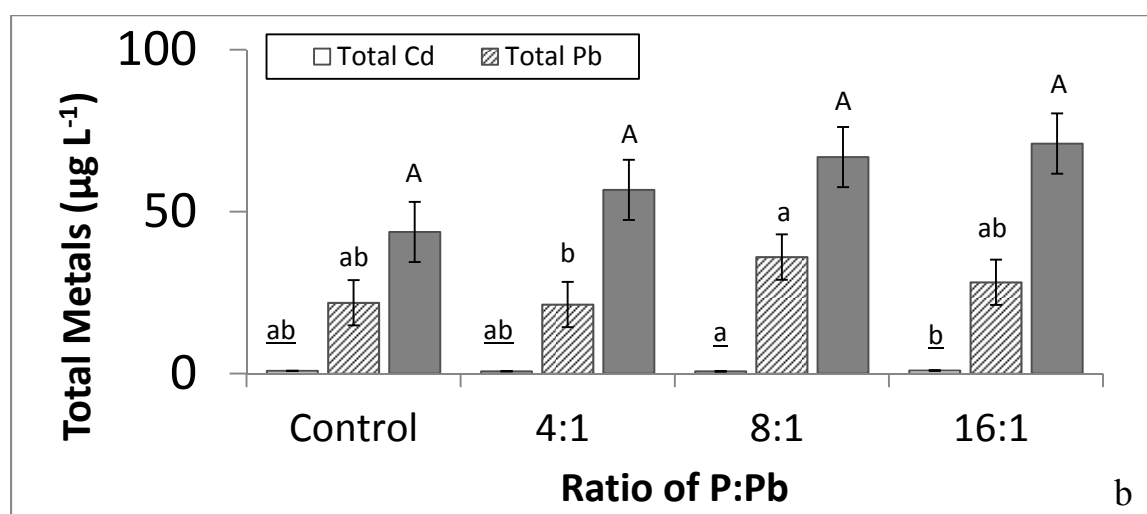
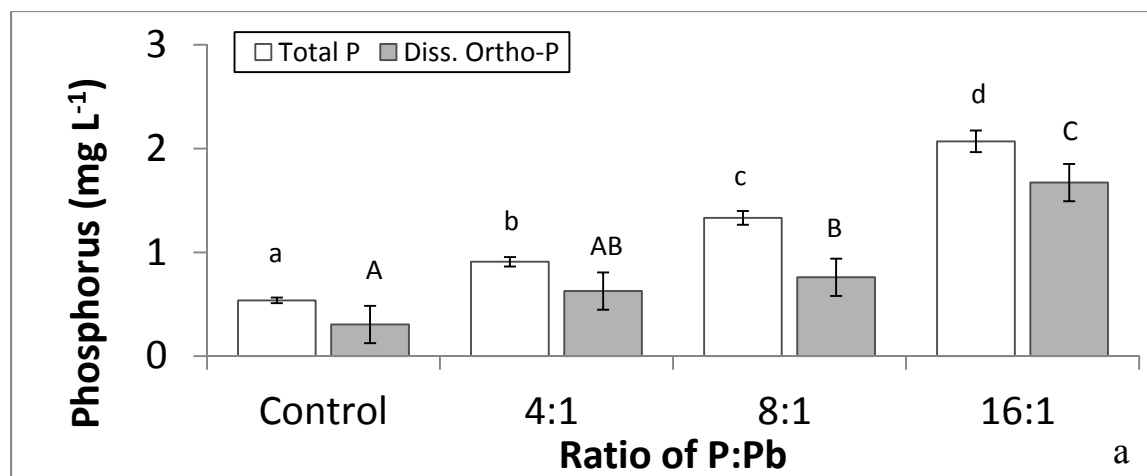


Figure 4. Water chemistry data from the second rainfall simulation including (a) total phosphorus and dissolved orthophosphate, (b) total metals, and (c) dissolved metals. Error bars represent standard error.

It is possible that the introduction of vegetation to the treatments may be responsible for some of the observed increases in effluent concentrations of dissolved Zn and Cd from the second RFS. Root exudates (*e.g.* low molecular weight organic acids) may play a role in release of Zn and Cd, but this was not investigated further in the current study.

Mass lost from second RFS was calculated using the same equation presented for RFS 1. Overall, the total mass of materials eroded during the second RFS was significantly less than those lost during the first RFS (Table 3, Fig. 5). The reduction in mass lost is especially pronounced for Pb (from 2.76 to 0.007 kg/ha at the 8:1 P:Pb ratio) and P (6.01 to 0.38 kg/ha at the 16:1 P:Pb ratio) The mass of eroded materials from the second RFS was insufficient to permit analysis of available P (Appendix D).

These results, in concert with the water quality results from the second RFS, strongly support the immediate establishment of vegetation on P treated soils to reduce potential eutrophication of proximal surface waters. The timing and tillage practices associated with P loss and application of manures demonstrate similar response patterns as our work (Schroeder et al., 2004). Consequently, the total picture of phosphorus, dissolved orthophosphate, total metals, and dissolved metals encourages us to recommend use of the lowest 4:1 P:Pb treatment class due to minimal P and reduced metals transport from the RFS test beds.

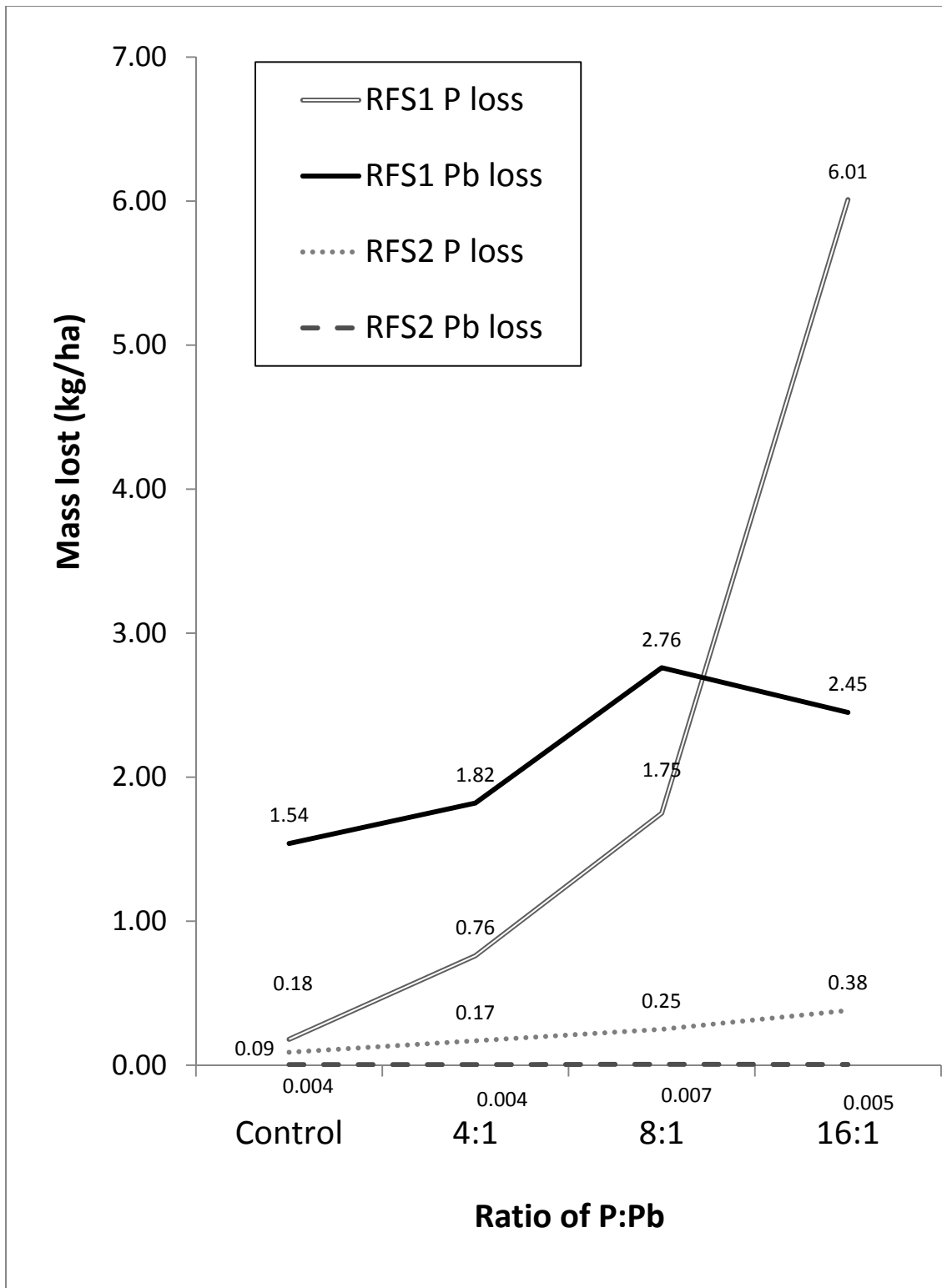


Figure 5. Mass of P and Pb lost during RFS1 compared to RFS2 in kilograms per hectare.

Influence of P treatment on Metals Uptake by Tall Fescue

In order to construct an investigation that accurately simulated potential field application conditions, the RFS boxes were vegetated with tall fescue (*Festuca arundinacea* Schreb; Kentucky 31) after the first RFS. As observed in Figure 6, Pb content within the plant tissues was significantly greater in the control (two- to nine-fold greater) relative to the P-treated soils after six months. No significant differences were observed between Pb content within the tissues of grass planted within the 4:1 and 8:1 P:Pb ratios, although Pb content of the tissues was nominally less in the 8:1 P:Pb treatment. Additionally, Pb content in the plants was significantly less in the soil treated with a 16:1 P:Pb ratio as compared to all other treatments. Nearly identical trends were observed for Pb concentration of plant tissues collected after 1 month of plant growth (Appendix C). Overall, the data demonstrate a significant reduction in plant bioavailable in Pb- contaminated soils treated with TSP that matches quite well with changes in Pb speciation observed in the XANES analysis, below.

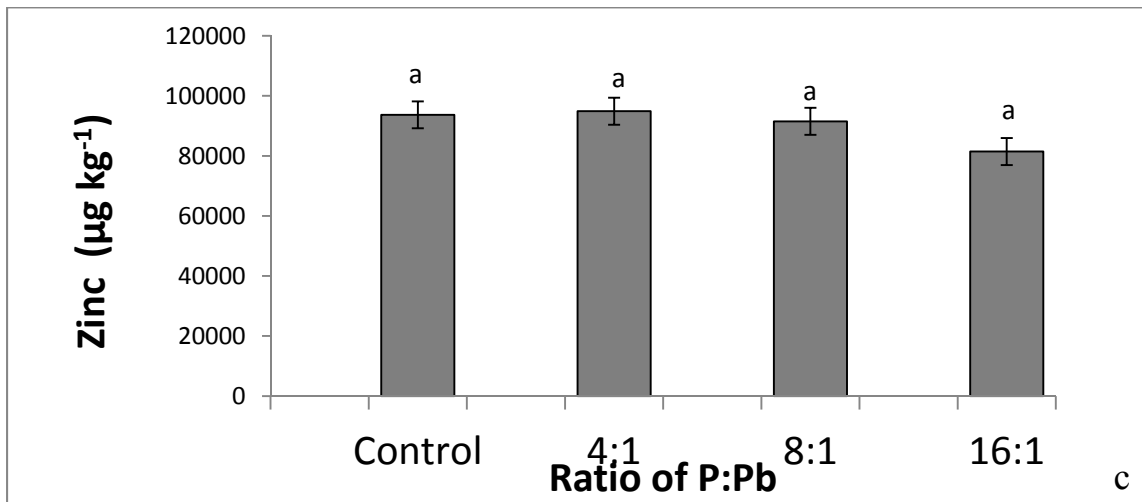
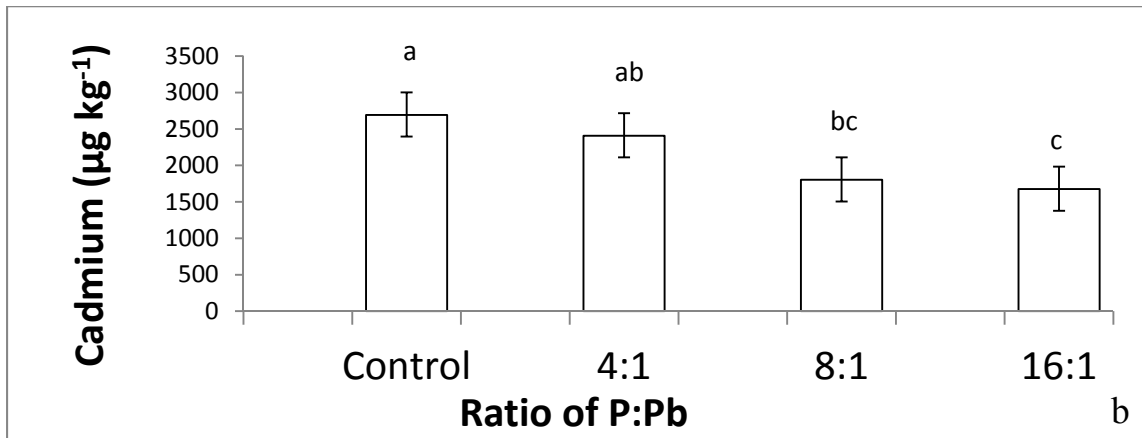
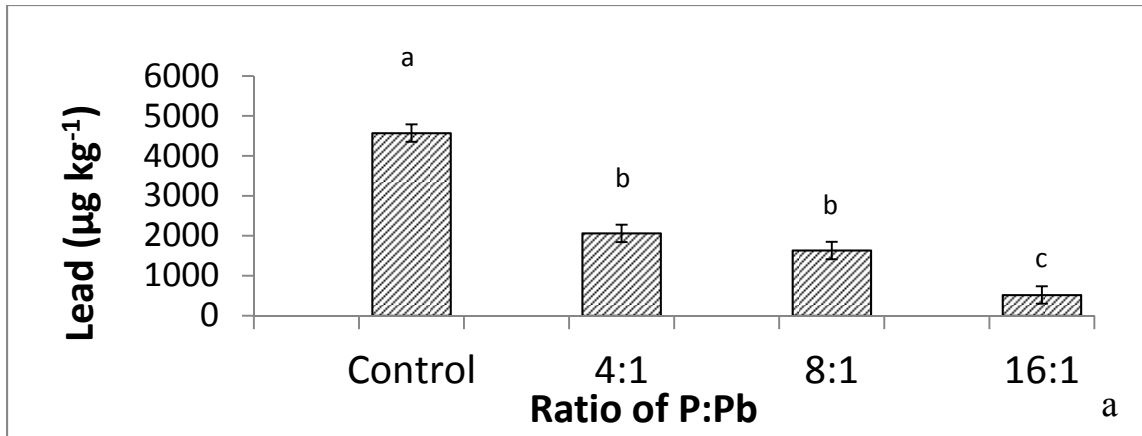


Figure 6. Arithmetic mean of elemental composition of above ground grass tissue six months after vegetation with tall fescue including (a) lead in grass tissue, (b) cadmium in grass tissue, and (c) zinc in grass tissue. Error bars represent standard error.

X-ray Absorption Near Edge Spectra and Linear Combination Fitting Analysis

The results of XANES analysis and linear combination fitting of standards to fit the XANES spectra are shown in Figure 7 for the un-amended control soil and selected P-treated soils following the RFS experiments. The LCF fits were developed utilizing reference spectra shown in Figure 8 and eliminating insignificant component reference spectra until the best statistical fit was acquired (Appendix E). For a lengthier description of the fitting procedure, see detailed accounts in Isaure et al. (2002), Roberts et al. (2002), and Scheinost et al. (2002).

Control samples

The predominant Pb species present in the control samples were plumbonacrite (38%) and plumboferrite (62%) (Table 4). These findings appear reasonable, as the source of Pb contamination to the floodplain of the Big River is attributed to crushed galena ores known to weather to Pb carbonate compounds such as plumbonacrite (Moles et al., 2004; Hillier et al., 2001; Cotter-Howells et al., 1994). Plumbonacrite is a poorly-crystalline precursor to hydrocerussite ($\text{Pb}_3(\text{CO}_3)_2(\text{OH})_2$) and cerussite (PbCO_3) (Krivovichev and Burns, 2000). The presence of plumboferrite in the control sample data are also consistent with soil Pb mineral assemblages near Leadville, CO where Pb associated with Fe oxides is thought to constitute more than 50% by mass of Pb species present (Ostergren et al., 1999; and Davis et al., 1993). Manganese and Fe-Pb oxides are known to occur in three forms from the soils at Leadville, CO, including discrete grains, coatings on non-Pb minerals, and as alteration rinds on Fe oxide particles (Davis et al., 1993).

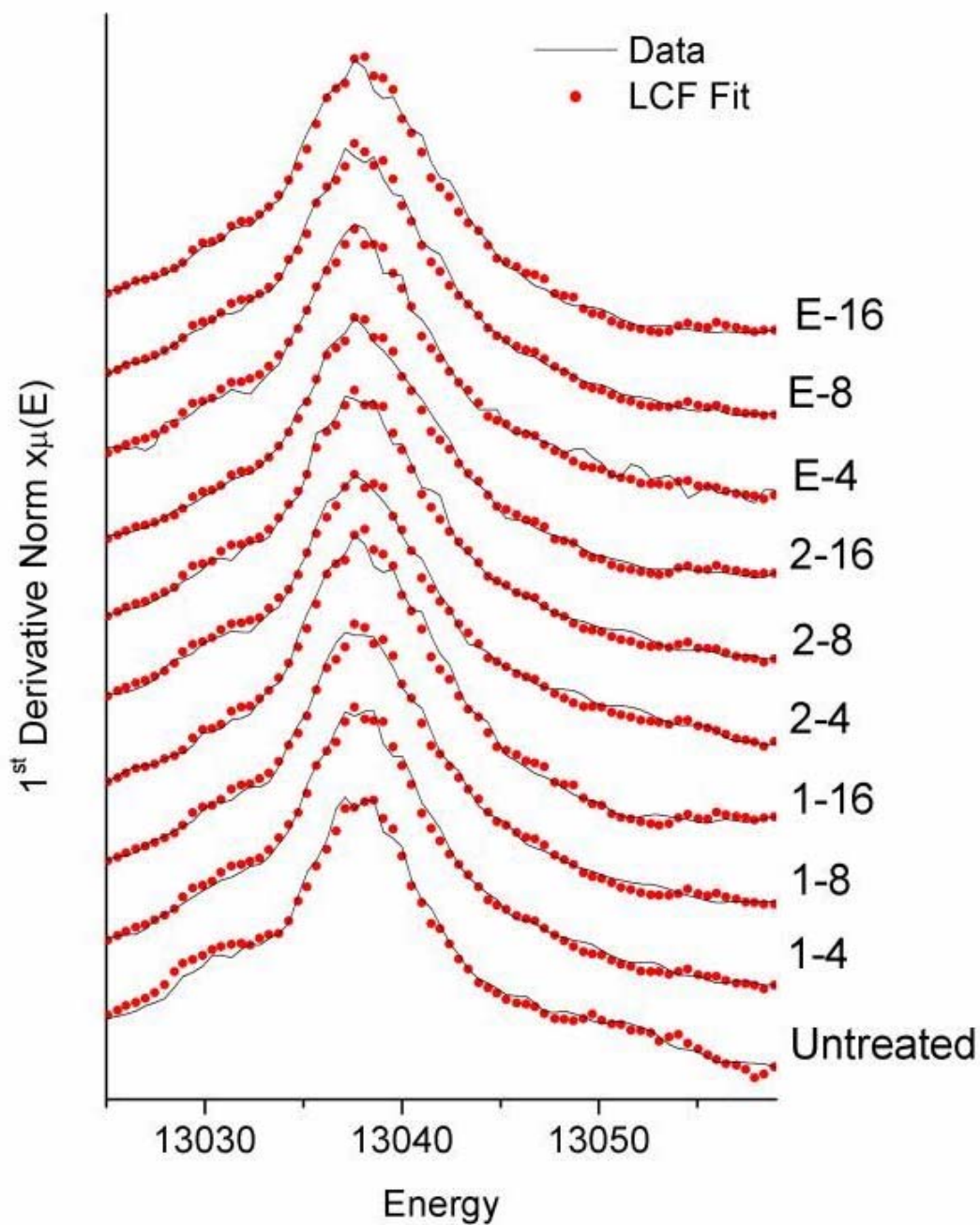


Figure 7. First derivative of normalized x-ray absorption near edge spectroscopy (XANES) spectra of untreated soils and select treated soils. The solid curve represents the raw sample data and the dotted curve are the fit results from linear combination of the reference spectra from Fig. 8.

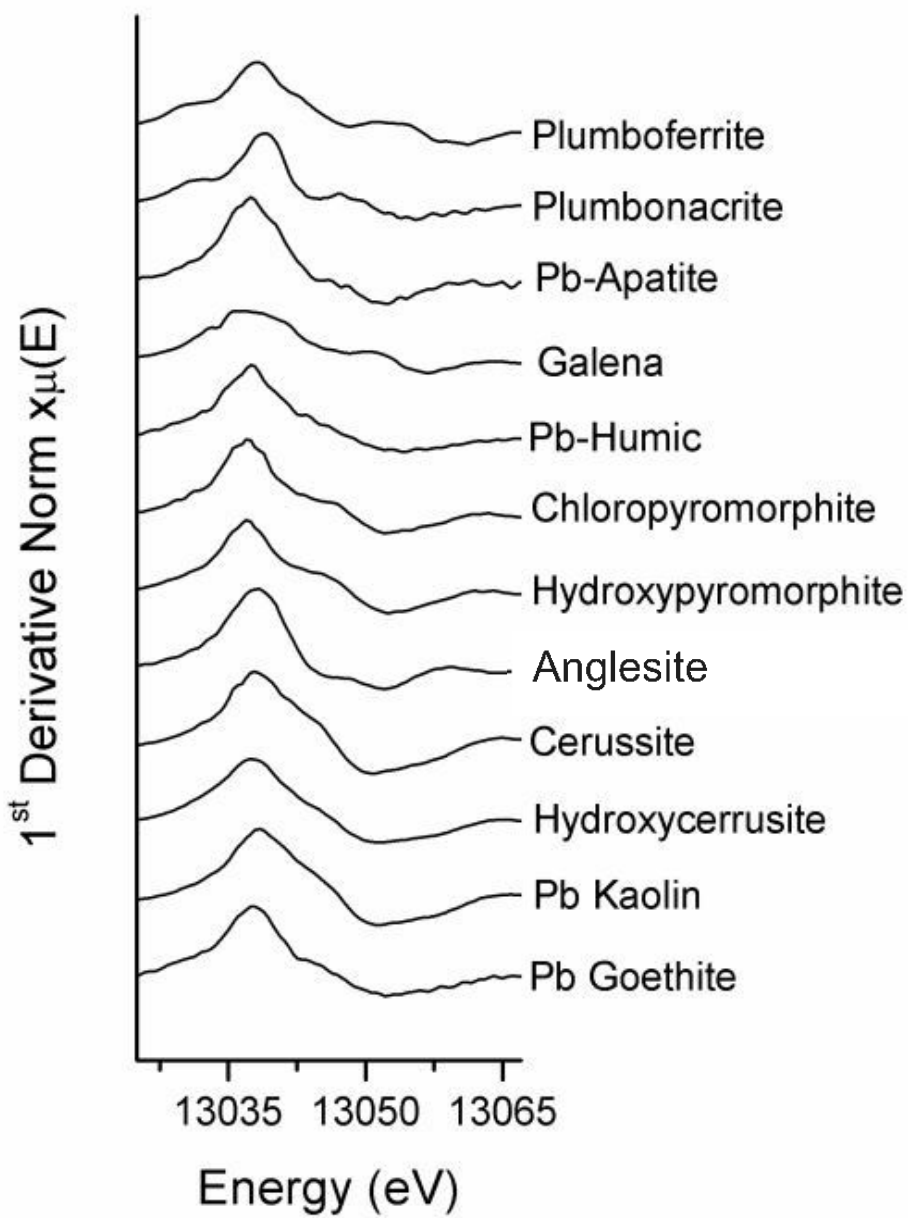


Figure 8. First derivative of normalized X-ray absorption near edge spectroscopy (XANES) spectra of reference samples employed as model components for linear combination fitting.

The nature of the association between Pb and Fe-rich materials has not been characterized in previous studies in southeast Missouri. These materials could contain Pb as microcrystalline precipitates or as adsorption complexes. Model system investigations suggest that Pb associated with Fe oxides is likely bound as adsorption complexes (Ford et al., 1997).

Phosphate amended samples from the first rainfall simulation

Control and treated soils were analyzed via XANES to quantify the species of Pb present in our experiment soils. Addition of TSP to the soil resulted in the transformation of up to 35% soil Pb to chloropyromorphite, concurrent with a dramatic decrease of plumbonacrite relative to Pb species within the control soil (Table 4 and Fig. 9). The amount of chloropyromorphite formed varied slightly, but not significantly, with TSP addition (29%, 4:1 and 16:1 P:Pb treatments; 35%, 8:1 P:Pb treatment). However, the addition of TSP to reach a molar ratio of 16:1 P:Pb appears to stimulate the formation of a Pb-sorbed to hydroxyapatite complex, which was absent from the control samples. While Pb within plumbonacrite appears to undergo complete transformation to other Pb-species (i.e., chloropyromorphite and Pb-hydroxyapatite complex), the relatively more insoluble plumboferrite continues to represent the major Pb species present in the treated soils following the first RFS event (Fig. 9).

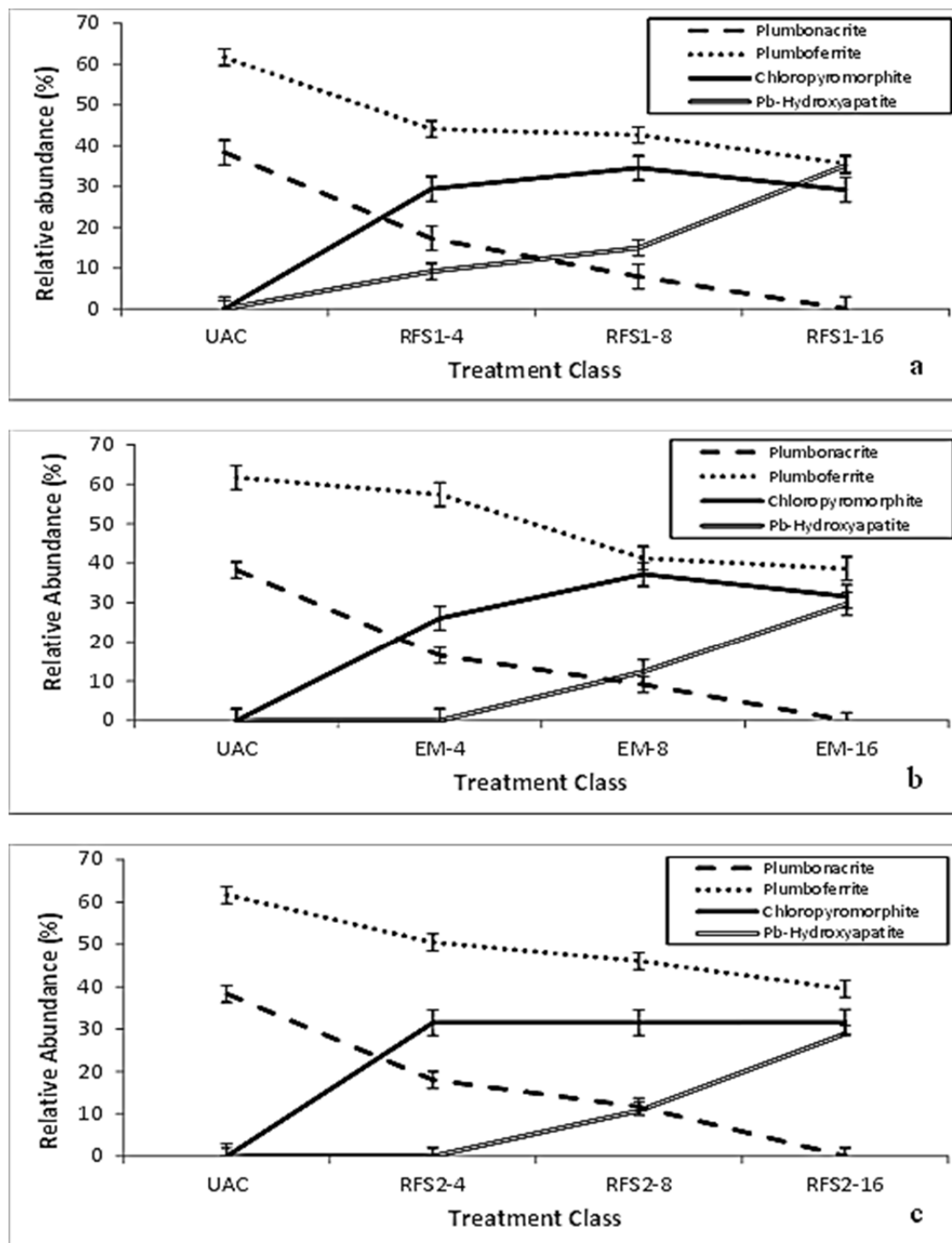


Figure 9. Relative abundance of Pb species in soils determined by an LCF model fitted to the XANES spectra at (a) first rainfall simulation, (b) in eroded material collected from effluents of first rainfall simulation, and (c) following second rainfall simulation. Error bars represent standard error. UAC is the un-amended control and EM is the eroded material.

Table 4. Linear combination fitting (LCF) results for X-ray absorption near edge spectroscopy (XANES) analysis of control and amended soil samples after rainfall simulation.

Sample ¹	Corrected Relative Abundance Determined by LCF Species								
	Plumbonacrite (%)	Error (%)	Plumboferrite (%)	Error (%)	Chloropyromorphite (%)	Error (%)	Pb sorbed to Hydroxyapatite (%)	Error (%)	R
UAC	38	2	62	2	0	0	0	0	0.0081
RFS1-4	17	3	44	2	29	3	9	2	0.0047
RFS1-8	8	3	43	2	35	3	15	3	0.0043
RFS1-16	0	0	36	2	29	4	35	2	0.0061
EM-4	17	4	57	4	26	4	0	0	0.0192
EM-8	9	3	41	2	37	3	12	3	0.0049
EM-16	0	0	39	3	32	3	30	3	0.0058
RFS2-4	18	2	50	2	32	2	0	0	0.0059
RFS2-8	12	3	46	2	32	4	11	3	0.0064
RFS2-16	0	0	40	2	32	3	29	2	0.0043

1: UAC, Un-amended control; RFS1-4, rainfall simulation 1, 4:1 P:Pb treatment class; RFS2-4, rainfall simulation 2, 4:1 P:Pb treatment class; EM-4, eroded material 4:1 P:Pb treatment class etc.

Material eroded from the un-vegetated RFS boxes was collected during the first RFS event and processed as described in section 2.3.7. Eroded materials were also analyzed using XANES and fitted with the LCF model. The resulting data follow a remarkably similar distribution to the samples described in the previous section (Fig. 9). The LCF model identified the greatest level of chloropyromorphite formation (37%) from our study at the 8:1 P:Pb treatment class in the eroded materials. Other transformations of Pb species are consistent with those observed from the soils collected from the RFS boxes following the first RFS.

Phosphate amended samples from the second rainfall simulation

Soil from the RFS test beds after the second RFS event and eroded materials collected during this event were also analyzed using XANES and modeled using LCF, and a similar distribution of abundance between the previously discussed Pb species was observed. The LCF model indicated that the soluble plumbonacrite was completely absent within soil treated with P to achieve a 16:1 P:Pb molar ratio, and plumboferrite was the most predominant Pb species (Table 4). Chloropyromorphite formation increased to 32% of Pb species present at the 4:1 P:Pb treatment level, which is identical to the amount of chloropyromorphite formed in samples receiving greater P application (8:1 and 16:1 P:Pb) (Fig. 9). Similar to XANES results from samples collected after the first RFS, the amount of the Pb-sorbed to hydroxyapatite species (29%) was greatest in 16:1 P:Pb treatment soil. Interestingly, the proportions of the Pb-hydroxyapatite species within soils collected after the second RFS study are consistently less than Pb-hydroxyapatite in samples collected after the first RFS study, and this reduction corresponds with slightly greater percentages of chloropyromorphite and plumboferrite. We

postulate that Pb is desorbed from the hydroxyapatite surface with time resulting, subsequently, in formation of other Pb species. Overall, this data suggests that TSP application required to achieve a 4:1 P:Pb ratio may be sufficient to trigger the greatest degree of pyromorphite formation over time. The overall percentages of chloropyromorphite formation at the 1 year (RFS2) time interval agree well with other recent studies utilizing TSP as the amending agent (Scheckel and Ryan, 2004; Ryan et al., 2001).

Overall trends from XANES analysis of soil samples

Similar TSP-based phosphorus amendments have been utilized in other studies (Scheckel and Ryan, 2004; Scheckel et al., 2005; Cao et al., 2002, 2003; Chen et al., 2003; Melamed et al., 2003), with a mixed picture of results for the transformation of Pb species. The earlier studies (Cao et al., 2002, 2003; Chen et al., 2003; Melamed et al., 2003) tended to report greater pyromorphite formation (70-82%) than the present study. However, later analysis by Scheckel and Ryan (2003; 2004) and Scheckel et al. (2005) demonstrated that the selective sequential extractions used in the earlier studies may cause the precipitation of pyromorphites during the extraction process. Percent of pyromorphite formation reported by Scheckel and Ryan (2004) and Scheckel et al. (2005) (29-41%) also using Pb contaminated Missouri soils and non-destructive synchrotron spectroscopic techniques compare favorably with the results reported here.

Our data demonstrating greater to complete dissolution of plumbonacrite with increased treatment levels of TSP differ from the data presented by Scheckel and Ryan (2004) and Scheckel et al., (2005) regarding the transformation of Pb species other than pyromorphites. Scheckel and Ryan (2004) report the complete transformation of galena (PbS) and partial

transformation of anglesite (PbSO_4) with marked increases in relative abundance of cerussite in soils treated with TSP compared to un-amended control samples. These differences can likely be explained by the species of Pb identified in our control samples prior to amendment: plumboferrite and plumbonacrite. Conversely, Pb species in the soils analyzed by Scheckel and Ryan (2004) consisted primarily of galena and anglesite in the un-amended control soils.

The marked increase in the formation of the Pb-sorbed to hydroxyapatite species in conjunction with observed plateau of chloropyromorphite formation represents an exciting possibility for future research in soil Pb/P chemistry. While all three classes of samples (RFS1, EM, and RFS2) demonstrate similar trends, the plateau of chloropyromorphite formation observed during analysis of the second RFS samples (Fig. 9) is particularly interesting. Previous studies report that chloropyromorphite formation occurs via a rapid kinetic reaction in phosphorus-amended soils, sometimes within a second to an hour (Zhang and Ryan, 1999). The plateau in pyromorphite formation combined with the formation and subsequent reduction of the Pb-hydroxyapatite complex over time, as well as the continued dissolution of the plumbonacrite suggests that Pb-hydroxyapatite formation did not reduce chloropyromorphite development. Instead, the data suggest that Pb may be desorbing from the hydroxyapatite surface with time (35% in RFS1 to 29% RFS2 at 16:1 P:Pb) and may form additional plumboferrite or chloropyromorphite.

The significantly reduced concentrations of dissolved P observed in the effluents from RFS2 (Fig. 5) may also play a role in limiting the formation of chloropyromorphite in soils. A lack of available P in the soil solution is known to halt the formation of pyromorphite (Cao et al., 2003) as is a lack of soluble Pb. Notably, we did not observe significant differences between the

treatments in the concentrations of dissolved Pb from RFS2, suggesting that the availability of soluble Pb is not the limiting reactant for the formation of pyromorphites.

It is also important to consider the role of pH in kinetic transformations. The transformation of Pb species into pyromorphite is dependent on the pH of the soil and this transformation is favored under acidic to weak acidic conditions (Xu and Schwartz, 1994; Zhang and Ryan, 1999). Other studies have not reported data for soil pH alteration upon the addition of acidic P amendments (*e.g.*, H₃PO₄ and TSP); but, the very high stoichiometric ratios of P:Pb used by Scheckel and Ryan (2004) suggest that soil acidification and favorable kinetic conditions for the formation of pyromorphites must have been present in the system. However, even under the most favorable stoichiometric and kinetic conditions created by Scheckel and Ryan (2004), the maximum level of pyromorphite formation achieved peaked at 45% when employing a 1% H₃PO₄ treatment. Accordingly, there must be other factors limiting the formation of pyromorphite in soils. Several studies (Hashimoto et al., 2009; Scheckel and Ryan, 2004) suggest that high organic matter levels in treated soils may control the activity of free Pb²⁺ species via formation of Pb- dissolved organic carbon complexes in solution and organic coatings on chloropyromorphite crystals which inhibit further transformation of Pb. Chappell and Scheckel (2007) also suggest a role for humic substances in the disproportionate transformation of the carbonate species to pyromorphite but do not discuss a full mechanism for this transformation. Although we cannot completely rule out the role of Pb sorption to organic matter as a limitation to further pyromorphite formation in the soils studied (OC = 21 g kg⁻¹), inclusion of a Pb-humic acid species did not improve the LCF model used to describe the XANES spectra.

Alternatively, the plateau in chloropyromorphite formation observed in our data and other studies may be attributable to the complexation of P with Al, Ca, Fe, and Mn in soil solution or P sorption to metal oxides. Aluminum and Fe oxides are known to have a great affinity for sorbing P, and may be sorbing P upon release into soil solution (Cao et al., 2002). Additionally, Hashimoto et al. (2007) reports that soils with abundant Al and Fe hydroxides tend to increase their ability to sorb anions at acidic pH conditions where the surface of the minerals is positively charged. Consequently, the creation of acidic pH soil conditions which kinetically favor the formation of pyromorphite may also induce the sorption of P to positively charged Al and Fe hydroxides as described by Hashimoto et al. (2009). The most acidic pH measured in this study was in soil from the 16:1 P:Pb treatment at 60 days post treatment ($\text{pH}_{\text{water}} = 5.43$, Appendix D) which is within a range favorable for pyromorphite formation as well as Al and Fe oxide protonation. Additionally, hydroxyapatite is known to selectively remove Pb from solution in the presence of aqueous metallic cations such as Al, Cd, Cu, Fe, Ni, or Zn (Ma et al., 1994b; Xu and Schwartz, 1994; Laperche et al., 1996). Thus, an abundance of dissolved metallic cations in conjunction with presence of hydroxyapatite may further explain limitations on the development of chloropyromorphite formed in this study. Several other studies (Ma et al., 1994b; Eighmy et al., 1997; and Crannell et al., 2000) suggest that the mechanism for the interference in the creation of pyromorphite is the formation of tertiary metal phosphates (*e.g.* $\text{Pb}_5(\text{PO}_4)_3\text{Cl}$ and $\text{Ca}_3(\text{PO}_4)_2$), or as ideal solid solutions (*e.g.*, $(\text{Pb}_2, \text{Ca})(\text{PO}_4)_2$).

Conclusions

The overall objective of this study was to determine if phosphorus (P) amendment technology could be implemented in an alluvial setting without releasing destructive quantities of P into nearby aquatic environments. To accomplish the overall objective, three specific goals were set at the initiation of the study: (1) determine the effect of variable treatment levels of P, treatment age, and vegetation on water quality; (2) evaluate the effect of P treatment on accumulation of metals in plant tissue; and (3) identify the P:Pb molar ratio treatment that results in the greatest level of pyromorphite formation. To meet these objectives, heavy metals contaminated alluvial soils from the floodplain of the Big River at Washington State Park in Jefferson County, Missouri, USA were amended with Triple Super Phosphate [TSP; $\text{Ca}(\text{H}_2\text{PO}_4)_2$] at one of four molar ratios of P to Pb (P:Pb): 0:1 (control); 4:1; 8:1; and 16:1. Following a six month reaction period, rainfall simulation (RFS) studies were initiated. Effluents from treated soils were collected during RFS events conducted at six months and one year post-treatment and analyzed to quantify total and dissolved P and Pb loss from the amended and un-amended soils. Accumulation of metals in the grass planted on the treatments was examined and speciation of the Pb compounds present before and after the treatments was investigated with X-ray absorption near edge spectroscopy (XANES) at the Advanced Photon Source of the Argonne National Laboratory.

As expected, the 16:1 P:Pb treatment class had a disproportionately higher amount of total and dissolved phosphorus in its effluent, especially from the first, un-vegetated RFS, where total P was found to be 36 times greater than the control soils and nine times greater than the 4:1 P:Pb treatment. The current study also demonstrated that a significantly greater quantity of metals are initially released into effluents by phosphorus treatment, again, especially from the

first, un-vegetated RFS at the two greatest P:Pb treatment classes (8:1 and 16:1). Given six months of time and coverage with a dense sod forming turf grass, levels of all analytes (total dissolved P, total and dissolved metals) dramatically decreased during the second RFS. Levels of total metals were reduced by two orders of magnitude and levels of total phosphorus were reduced by one order of magnitude. Levels of dissolved phosphorus and dissolved Pb were reduced by approximately one half. Significantly, levels of dissolved Zn and Cd increased from RFS1 to RFS2 by two to four times their original values, suggesting an undesirable outcome for these more soluble metals.

When total losses of contaminants of concern were calculated and the data from each RFS were compared, we observed significant reductions from the RFS1 to RFS2 across every analyte considered here. Total P concentrations and loss in the effluents from RFS was least in the 4:1 P:Pb ratio treatment among the P-treated soils, and total Pb concentration and mass lost was comparable between the control and 4:1 P:Pb ratio before and after the establishment of vegetation following RFS1. From the effluent data, we are lead to recommend the lowest P:Pb treatment class (4:1) as the most advisable given its effluent data indicating the lowest concentrations of all undesirable measured analytes of concern.

As an additional line of evidence to evaluate the P treatment classes, grass tissues from control and treated plots were analyzed for total metals. Pb content within the plant tissues was significantly greater in the control (two- to nine-fold greater) relative to the P-treated soils. Additionally, Pb content in the plants was significantly less in the soil treated with a 16:1 P:Pb ratio as compared to all other treatments. Overall, the data demonstrate a significant reduction in the bioavailability of Pb minerals in the soil which agree with the changes in Pb speciation observed in the XANES analysis.

Where the ultimate goal of treating Pb contaminated soils is the creation of highly insoluble pyromorphite compounds, our data suggest that, in the limited time range (1 year) considered, the lowest P:Pb treatment level considered (4:1) is sufficient to create chloropyromorphite equivalent to the highest P:Pb treatment class (16:1) in this soil. Approximately 32% of the Pb present in the soils after 1 year was successfully converted to chloropyromorphite at all P:Pb molar ratio treatments studied. This plateau effect in the creation of chloropyromorphite in combination with the exceptionally high levels of phosphorus reported in the effluents from the 16:1 P:Pb treatment class during the initial RFS (mean =36.15 mg L⁻¹) suggest that the 4:1 P:Pb treatment level could be implemented with an equal likelihood of success for the conversion of Pb species to less bioavailable forms. Peak levels of Pb species transformation to pyromorphites in this study compare well with other studies employing similar methodology and analyses (Scheckel and Ryan, 2004; Scheckel et al., 2005; Yang et al., 2001).

The observed plateau in the formation of chloropyromorphite also suggests that other factors in the soil solution are controlling the formation of the desired Pb species beyond the simple availability of free phosphate ions. The marked increase in the concentrations of the Pb-sorbed to hydroxyapatite compound at the 16:1 P:Pb treatment level throughout our experiment suggest that further additions of phosphorus in a calcium rich environment may not promote additional formation of pyromorphite; instead intermediary or perhaps precursors to pyromorphites are formed, as suggested by Chappell and Scheckel (2007). Additionally, the role of pH and humic substances in controlling the favorability of Pb speciation in a slightly alkaline environment is only lightly considered in this study; and our understanding of the present soil solution chemistry could be greatly enhanced with further analysis of their effect on the surface chemistry of soil minerals present. It would be illuminating to examine the very same soils with

XANES analyses at two and three years' post treatment. An extension of the period of evaluation for this soil and treatments should reveal the eventual fate and transformation of Pb species observed in this limited time frame.

Management Recommendations

As a consequence of the multiple lines of evidence generated by this experiment including effluent and soil chemistry from RFS, direct measurement of Pb uptake in plants, and speciation via XANES, the use of the 4:1 P:Pb ratio treatment class is recommended. The 4:1 P:Pb ratio treatment class, out of the full range of P treatment ratios considered for this soil, is the option with the greatest likelihood of success in the desired reduction in bioavailability of Pb species present with the lowest likelihood of potential negative environmental consequences.

Future Research

This project represents the first phase of a two phase process to assess the environmental implications of implementing P amendments in a metals contaminated floodplain. The next step within this domain of soils and environmental research is to implement P-treatment on a pilot study scale at the site of contaminated floodplain soils and to measure the concentrations of metals and nutrients eluted during actual, not simulated, precipitation events. Operation of a pilot level study with passive runoff sampling equipment over multiple years in conjunction with metals speciation via XANES may answer the majority of remaining questions regarding the environmental sustainability and pollution potential of phosphorus based remedial technologies. Research describing P and Pb runoff from *in situ* plots in Pb-contaminated soils treated with P does not exist at this time. Research evaluating the effectiveness of vegetative buffer strips and other P best management practices in sequestration of the potential runoff from such sites also

does not exist, and would fill a necessary void in our understanding of conditions likely encountered during implementation of such a remedy. When completed, this potential future research will serve to answer many of the remaining questions and allow for the initiation of P-based remediation.

References

- Arnich N, M.C. Lanhers, F. Laurensot, R. Podor, A. Montiel, and D. Burnel. 2003. In vitro and in vivo studies of lead immobilization by synthetic hydroxyapatite. *Environ. Pollut.* 124:139–149.
- Basta, N.T., and S.L. McGowen. 2004. Evaluation of chemical immobilization treatments for reducing heavy metal transport in a smelter-contaminated soil. *Environ. Pollut.* 127:73–82.
- Beyer, W. N., J. Dalgarn, S. Dudding, J.B. French, R. Mateo, J. Miesner, L. Sileo, and J. Spann. 2005. Zinc and lead poisoning in wild birds in the Tri-State Mining District (Oklahoma, Kansas, and Missouri). *Arch. Environ. Contam. Toxicol.* 48:108-117.
- Blanco-Canqui, H., C.J. Gantzer, S.H. Anderson, E.E. Alberts, and A.L. Thompson. 2004. Grass barrier and vegetative filter strip effectiveness in reducing runoff, sediment, nitrogen, and phosphorus loss. *Soil Sci. Soc. Am. J.* 68:1670–1678.
- Cao, X., L.Q. Ma, M. Chen, S.P. Singh, and W.G. Harris. 2002. Impacts of phosphate amendments on lead biogeochemistry at a contaminated site. *Environ. Sci. Technol.* 36:5296–5304.
- Cao, R.X., L.Q. Ma, M. Chen, S.P. Singh, and W.G. Harris. 2003. Phosphate-induced metal immobilization in a contaminated site. *Environ. Pollut.* 122:19–28.
- Casteel, S.W., R.W. Blanchar, and J. Yang. 1997. Effect of phosphate treatment on the bioavailability of lead from the Jasper County site—Joplin, Missouri. Missouri Department of Natural Resources, Jefferson City, MO.
- CDC (Centers for Disease Control). 2012. Low level lead exposure harms children: A renewed call for primary prevention. Atlanta, GA: U.S. Department of Health and Human Services, Centers for Disease Control and Prevention.
- Chappell, M.A. and K.G. Scheckel. 2007. Pyromorphite formation and stability after quick lime neutralization in the presence of soil and clay sorbents. *Environ. Chem.* 4:109-113.
- Chen, S.B., Y.G. Zhu, and Y.B. Ma. 2006. The effect of grain size of rock phosphate amendment on metal immobilization in contaminated soils. *J. Hazard. Mater.* 134:74–79.
- Chrysochoou, M., D. Dermatas, and D.G. Grubb. 2007. Phosphate application to fire range soils for Pb immobilization: The unclear role of phosphate. *J. Hazard. Mat.* 144:1-14.
- Cotter-Howells, J. D., P.E. Champness, J.M. Chamock, and R.P. Patrick. 1994. Identification of pyromorphite in mine-waste contaminated soils by ATEM and EXAFS. *Eur. J. Soil Sci.* 45: 393–402.

- Crannell, B.S., T.T. Eighmy, J.E. Krzanowski, J.D. Eusden Jr, E.L. Shaw, and C.A. Francis. 2000. Heavy metal stabilization in municipal solid waste combustion bottom ash using soluble phosphate. *Waste Management* 20:135–148.
- Davis, A., J.W. Drexler, M.V. Ruby, and A. Nicholson. 1993. Micromineralogy of mine wastes in relation to lead bioavailability, Butte, Montana. *Environ. Sci. Technol.* 27:1415–1425.
- Dermatas, D., M. Chrysochoou, D.G. Grubb, and X. Xu. 2008. Phosphate treatment of firing range soils: lead fixation or phosphorus release. *J. Environ. Qual.* 37:47–56.
- Eighmy T.T., B.S. Crannell, L. Butler, F.K. Cartledge, E.F. Emery, D. Oblas, J.E. Krzanowski, J.D. Eusden Jr, E.L. Shaw, and C.A. Francis. 1997. Heavy metal stabilization in municipal solid waste combustion dry scrubber residue using soluble phosphate. *Environ. Sci. Technol.* 31:3330–3333
- Eisler, R. 1988. Lead hazards to fish, wildlife, and invertebrates: a synoptic review. U.S. Fish Wildl. Serv. Biol. Rep. 85(1.14).
- Ford, R.G., P.M. Bertsch, and K.J. Farley. 1997. Changes in transition and heavy metal partitioning during hydrous iron oxide aging. *Environ. Sci. Technol.* 31: 2028-2033.
- Hashimoto, Y., T.J. Smyth, D. Hesterberg, and D.W. Israel. 2007. Soybean root growth in relation to ionic composition in magnesium-amended acid subsoils: implications on root citrate ameliorating aluminum constraints. *Soil Sci. Plant Nutr.* 53: 753–763.
- Hashimoto, Y., M. Takaoka, K. Oshita, and H. Tanida. 2009. Incomplete transformations of Pb to pyromorphite by phosphate induced immobilization investigated by X-ray absorption fine structure (XAFS) spectroscopy. *Chemosphere* 76:616-622.
- Hettiarachchi, G.M., G.M. Pierzynski, and M.D. Ransom. 2001. In situ stabilization of soil lead using phosphorus. *J. Environ. Qual.* 30:1214–1221.
- Hillier, S. K. Suzuki, and J. Cotter-Howells. 2001. Quantitative determination of cerussite by X-ray powder diffraction and inferences for lead speciation and transport in stream sediments from a former lead mining area in Scotland. *Applied Geochem* 6:597-608.
- Isaure, M.-P., A. Laboudigue, A. Manceau, G. Sarret, C. Tiffreau, P. Trocellier, G. Lambelle, J.-L. Hazemann, and D. Chateigner. 2002. Quantitative Zn speciation in a contaminated dredged sediment by μ -PIXE, μ -SXRF, EXAFS spectroscopy and principal component analysis. *Geochim. Cosmochim. Acta* 66:1549–1567.
- Kilgour, D. W., R.B. Moseley, M.O. Barnett, K. S. Savage, and P.M. Jardine. 2008. Potential negative consequences of adding phosphorus-based fertilizers to immobilize lead in soil. *J. Environ. Qual.* 37: 1733–1740.

- Krivovichev, S.V., and P.C. Burns. 2000. Crystal chemistry of basic lead carbonates. II. Crystal structure of synthetic plumbonacrite. *Mineral. Mag.* 64(6): 1069-1075.
- Laperche, V., S.J. Traina, P. Gaddam, and T.J. Logan. 1996. *In situ* immobilization of lead in contaminated soils by synthetic hydroxyapatite: chemical and mineralogical characterizations. *Environ. Sci. Technol.* 30:3321–3326.
- Lewin, M.D., S. Sarasua, and P.A. Jones. 1999. A multivariate linear regression model for predicting children's blood lead levels based on soil lead levels: a study at four superfund sites. *Environmental Research Section A* 81, 52-61.
- Ma, Q.Y., S.J. Traina, and T.J. Logan. 1993. *In situ* lead immobilization by apatite. *Environ. Sci. Technol.* 27:1803–1810.
- Ma, Q.Y., Traina, S.J., Logan, T.J., and Ryan, J.A. 1994. Effects of Aqueous Al, Cd, Cu, Fe(II), Ni, and Zn on Pb Immobilization by Hydroxyapatite. *Environ. Sci. Technol.* 28: 1219- 1228.
- Ma, Q.Y., T.J. Logan, and S.J. Traina. 1995. Lead immobilization from aqueous solutions and contaminated soils using phosphate rocks. *Environ. Sci. Technol.* 29:1118–1126.
- Melamed, R., X. Cao, M. Chen, and L. Ma. 2002. Field assessment of lead immobilization in a contaminated soil after phosphate application. *Sci. Tot. Environ.* 305: 17-127.
- Moles, N.R., D. Smyth, C.E. Maher, E.H. Beattie, and M. Kelly. Dispersion of cerussite-rich tailings and plant uptake of heavy metals at historical lead mines near Newtownards, Northern Ireland. *Applied Earth Sci.* 113(1): 21-30.
- Ostergren, J.D., G.E. Brown, G.A. Parks, and T.N. Tingle. 1999. Quantitative Speciation of Lead in Selected Mine Tailings from Leadville, CO. *Environ. Sci. Technol.* 33:1627-1636.
- Pavlovsky, R. 2010. Distribution, geochemistry, and storage of mining sediment in channel and floodplain deposits of the Big River system in St. Francois, Washington, and Jefferson Counties, Missouri. The Ozarks Environmental and Water Resources Institute, Missouri State University, Springfield, MO.
- Ravel, B.; Newville, M. Athena, Artemis, Hephaestus: data analysis for X-ray absorption using IFEFFIT. *J. Synchrotron Radiat.* 2005, 12, 537-541
- Roberts, D.R., A.C. Scheinost, and D.L. Sparks. 2002. Zn speciation in a smelter contaminated soil profile using bulk and micro-spectroscopic techniques. *Environ. Sci. Technol.* 36:1742–1750
- Ruby, M.V., A. Davis, and A. Nicholson. 1994. *In situ* formation of lead phosphates in soils as a method to immobilize lead. *Environ. Sci. Technol.* 28:646–654

- Ryan, J.A., P.C. Zhang, D. Hesterberg, J. Chou, and D.E. Sayers. 2001. Formation of chloropyromorphite in a lead-contaminated soil amended with hydroxyapatite. *Environ. Sci. Technol.* 35:3798–3803
- Salatas, J.H., Y.W. Lowney, R.A. Pastorok, R.R. Nelson, and M.V. Ruby. 2004. Metals that drive health-based remedial decisions for soils at U.S. Department of Defense sites. *Hum. Ecol. Risk Assess.* 10:983–997.
- Scheckel, K. G., Impellitteri, C. A., Ryan, J. A. and T. McEvoy. 2003. Assessment of a sequential extraction procedure for perturbed lead-contaminated samples with and without phosphorus amendments. *Environ. Sci. Technol.* 37: 1892–1898.
- Scheckel, K. G., Ryan, J. A., Allen, D. and N.V. Lescano. 2005. Determining speciation of Pb in phosphate-amended soils: Method limitations. *Sci. Total Environ.* 350: 261–272.
- Scheckel, K. G. and J.A. Ryan. 2002. Effects of aging and pH on dissolution kinetics and stability of chloropyromorphite. *Environ. Sci. Technol.* 36: 2198–2204.
- Scheckel, K.G., and J.A. Ryan. 2003. In vitro formation of pyromorphite via reaction of Pb sources with soft-drink phosphoric acid. *Sci. Total Environ.* 302:253–265.
- Scheckel, K.G., and J.A. Ryan. 2004. Spectroscopic Speciation and Quantification of Lead in Phosphate-Amended Soils. *J. Environ. Qual.* 33:1288-1295.
- Scheinost, A.C., R. Kretzschmar, and S. Pfister. 2002. Combining selective sequential extractions, X-ray absorption spectroscopy, and principal component analysis for quantitative zinc speciation in soil. *Environ. Sci. Technol.* 36:5021–5028.
- Schroeder, P.D., D.E. Radcliffe, and M.L. Cabrera. 2004 Rainfall timing and poultry litter application rate effects on phosphorus loss in surface runoff. *J. Environ. Qual.* 33:2201-2209.
- Seeger, C.M. 2008. History of mining in the southeast Missouri lead district and description of mine processes, regulatory controls, environmental effects, and mine facilities in the Viburnum trend subdistrict. In Kleeschulte, M.J., ed., 2008, *Hydrologic investigations concerning lead mining issues in southeastern Missouri: U.S. Geological Survey Scientific Investigations Report 2008–5140*, Chapter 1.
- Sharpley A.N. and A.D. Halvorson 1994. The management of soil phosphorus availability and its impact on surface water quality. In: Lal R, Stewart BA (eds) *Soil processes and water quality*. Lewis, Boca Raton, FL, pp 7–90.
- Sarpley, A.N. and P. Kleinman. 2003. Effect of rainfall simulator and plot scale on overland flow and phosphorus transport. *J. Environ. Qual.* 32:2172–2179.
- Sims J.T. 1993. Environmental soil testing for phosphorus. *J. Prod. Agric.* 6:501–507.

- Spuller, C., H. Weigand, and C. Marb. 2007. Trace metal stabilisation in a shooting range soil: Mobility and phytotoxicity. *J. Hazard. Mater.* 141:378–387.
- Stanforth, R., and J. Qiu. 2001. Effect of phosphate treatment on the solubility of lead in contaminated soil. *Environ. Geol.* 41:1–10.
- Tang, X. J. Yang, K.W. Goyne, and B. Deng. 2009. Long-term risk reduction of lead-contaminated urban soil by phosphate treatment. *Env. Eng. Sci.* 26(12): 1747-1754.
- Theis, T.L., and P.J. McCabe. 1978. Phosphorus dynamics in hypereutrophic lake sediments. *Water Res.* 12:677-685.
- USEPA. 1993. Engineering Evaluation/Cost Analysis for the Big River Mine Tailings Site, Desloge, Missouri. U.S. Environmental Protection Agency, Region 7, Kansas City, KS.
- USEPA. 2007. The use of soil amendments for remediation, revitalization and reuse. Washington, DC: Office of Solid Waste and Emergency Response, U.S. Environmental Protection Agency. EPA 542-R-07-013.
- USEPA, 2007b. Method 365.1 Phosphorus, all forms (colorimetric, ascorbic acid, two reagent). Accessed at http://water.epa.gov/scitech/methods/cwa/bioindicators/upload/2007_07_10_methods_method_365_3.pdf. On 10 Oct 2012.
- USEPA, 2012b. Method 3052 Microwave assisted acid digestion of siliceous and organically based matrices. Accessed at <http://www.epa.gov/osw/hazard/testmethods/sw846/pdfs/3052.pdf>. On 15 Jan 2013.
- Xu, Y., and F.W. Schwartz. 1994. Lead immobilization by hydroxyapatite in aqueous solutions. *J. Contam. Hydrol.* 15:187–206.
- Yang, J., D. Mosby, S.W. Casteel, and R.W. Blanchar. 2001. Lead immobilization using phosphoric acid in a smelter-contaminated soil. *Environ. Sci. Technol.* 35:3553–3559.
- Yang, J., D. Mosby, S.W. Casteel, and R.W. Blanchar. 2002. *In vitro* lead bioaccessibility and phosphate leaching as affected by surface application of phosphoric acid in lead-contaminated soil. *Environ. Contam. Toxicol.* 43, 399–405.
- Yang J., and X. Tang. 2007. Water quality and ecotoxicity as influenced by phosphate treatments in metal-contaminated soil and mining wastes. *Environ. Monitor. Restor.* 3: 21-33.
- Zhang, P.C., J.A. Ryan, and J. Yang. 1998. *In vitro* soil solubility in the presence of hydroxyapatite. *Environ. Sci. Technol.* 32:2763–276

Zhang, P., and J. A. Ryan. 1999. Transformation of Pb(II) from cerussite to chloropyromorphite in the presence of hydroxyapatite under varying conditions of pH. *Environ. Sci. Technol.* 33: 625-630.

APPENDICES

APPENDIX A. SOIL PHOSPHORUS DOSING CALCULATIONS AND X-RAY FLUORESCENCE RESULTS

- TSP = 45% P₂O₅ by mass
- 1 mol P = 30.97 g
- P=30.97 g/mol x 2 = 61.94 g
- O=15.99 g/mol x 5 =79.95 g
- P₂O₅ = 141.89 g/mol
- P in P₂O₅= 61.94/141.89 = 43.65% P by mass
- 0.4365 x 0.45 in TSP = 0.1964 of 19.64% P in TSP by mass
- 100 g of TSP = 19.64 g P
- 157.69 g of TSP = 1 mol P

Mean Soil Concentration of Pb in Washington State Park Soil: 2119 mg kg⁻¹ (From Table 1).

$$\frac{2.119 \text{ g Pb}}{1 \text{ kg soil}} \times \frac{1 \text{ mol Pb}}{207.2 \text{ g Pb}} = 0.0102 \text{ mol Pb/kg soil}$$

$$\frac{0.0102 \text{ mol Pb}}{1 \text{ kg soil}} \times \frac{8 \text{ mol P}}{1 \text{ mol Pb}} \times \frac{157.69 \text{ g TSP}}{1 \text{ mol P}} = 12.87 \text{ g TSP kg}^{-1} \text{ soil} \quad 1:8 \text{ Pb: P Ratio}$$

- 1389.96 g TSP were added to 108 kg of air dried soil to achieve the 1:8 Pb:P ratio on April 11, 2012.

$$\frac{0.0102 \text{ mol Pb}}{1 \text{ kg soil}} \times \frac{4 \text{ mol P}}{1 \text{ mol Pb}} \times \frac{157.69 \text{ g TSP}}{1 \text{ mol P}} = 6.43 \text{ g TSP kg}^{-1} \text{ soil} \quad 1:4 \text{ Pb: P Ratio}$$

- 694.44 g TSP were added to 108 kg of air dried soil to achieve the 1:4 Pb:P ratio on April 11, 2012.

$$\frac{0.0102 \text{ mol Pb}}{1 \text{ kg soil}} \times \frac{2 \text{ mol P}}{1 \text{ mol Pb}} \times \frac{157.69 \text{ g TSP}}{1 \text{ mol P}} = 3.22 \text{ g TSP kg}^{-1} \text{ soil} \quad 1:2 \text{ Pb: P Ratio}$$

- 347.46 g TSP were added to 108 kg of air dried soil to achieve the 1:2 Pb:P ratio on April 11, 2012.

Table A.1. Washington State Park soil x-ray fluorescence results

SAMPLE ID	Pb (mg kg ⁻¹)	2 Standard Deviations (mg kg ⁻¹)	Zn (mg kg ⁻¹)	2 Standard Deviations (mg kg ⁻¹)
WSP-XRF-1	2063	63	639	45
WSP-XRF-1	2165	65	635	45
WSP-XRF-1	2125	64	681	47
MEAN	2118	64	652	46
WSP-XRF-2	2155	64	589	44
WSP-XRF-2	2127	65	596	45
WSP-XRF-2	2174	65	608	44
MEAN	2152	65	598	44
WSP-XRF-3	2051	62	560	42
WSP-XRF-3	2060	63	621	45
WSP-XRF-3	2111	63	617	44
MEAN	2074	63	599	44
WSP-XRF-4	2174	65	614	44
WSP-XRF-4	2118	64	661	46
WSP-XRF-4	2067	63	602	44
MEAN	2120	64	626	45
WSP-XRF-5	2093	64	627	45
WSP-XRF-5	2036	63	577	43
WSP-XRF-5	2218	65	603	44
MEAN	2116	64	602	44
WSP-XRF-6	2201	66	622	45
WSP-XRF-6	2156	65	639	46
WSP-XRF-6	2158	65	643	46
MEAN	2172	65	635	45
WSP-XRF-7	2141	65	615	45
WSP-XRF-7	2112	64	600	44
WSP-XRF-7	2092	64	636	46
MEAN	2115	64	617	45
WSP-XRF-8	2079	63	614	45
WSP-XRF-8	2098	64	624	45
WSP-XRF-8	2047	63	638	46
MEAN	2075	63	625	45
WSP-XRF-9	2221	66	606	45
WSP-XRF-9	2047	63	645	46
WSP-XRF-9	2093	63	610	44
MEAN	2120	64	620	45
WSP-XRF-10	2115	64	657	46
WSP-XRF-10	2141	66	716	49
WSP-XRF-10	2134	64	634	45
MEAN	2130	65	669	47
MEAN	2119	64		

APPENDIX B. RAINFALL SIMULATION CALIBRATION DATA.

Table B.1. Rainfall simulation calibration data and calculations

11/14/2012

Bucket	Full Mass (g)	Bucket Tare Mass (g)	Water Mass (g)	Catchment Area (cm²)	10 min Rainfall Rate (cm hour⁻¹)	1 hour Rainfall Rate (cm hour⁻¹)
CB1	350.17	83.87	266.3	323.65	0.8228	4.9367
CB2	368.39	83.01	285.38	323.65	0.8817	5.2905
CB3	338.66	83.89	254.77	323.65	0.7872	4.7230
CB4	373.93	84.00	289.93	323.65	0.8958	5.3748
CB5	373.6	85.95	287.65	323.65	0.8888	5.3325
CB6	334.71	83.14	251.57	323.65	0.7773	4.6637
CB7	369.63	82.69	286.94	323.65	0.8866	5.3194
					MEAN	5.0915

11/15/2012

Bucket	Full Mass (g)	Bucket Tare Mass (g)	Water Mass (g)	Catchment Area (cm²)	10 min Rainfall Rate (cm hour⁻¹)	1 hour Rainfall Rate (cm hour⁻¹)
CB1	335.34	83.87	251.47	323.65	0.7770	4.6618
CB2	377.08	83.01	294.07	323.65	0.9086	5.4516
CB3	376.85	83.89	292.96	323.65	0.9052	5.4310
CB4	396.68	84.00	312.68	323.65	0.9661	5.7965
CB5	336.48	85.95	250.53	323.65	0.7741	4.6444
CB6	356.9	83.14	273.76	323.65	0.8458	5.0750
CB7	359.74	82.69	277.05	323.65	0.8560	5.1360
					MEAN	5.1709

11/15/2012

Bucket	Full Mass (g)	Bucket Tare Mass (g)	Water Mass (g)	Catchment Area (cm²)	10 min Rainfall Rate (cm hour⁻¹)	1 hour Rainfall Rate (cm hour⁻¹)
CB1	320.31	83.87	236.44	323.65	0.7305	4.3832
CB2	351.24	83.01	268.23	323.65	0.8288	4.9725
CB3	389.66	83.89	305.77	323.65	0.9447	5.6684
CB4	332.42	84.00	248.42	323.65	0.7675	4.6053
CB5	367.48	85.95	281.53	323.65	0.8698	5.2191
CB6	367.47	83.14	284.33	323.65	0.8785	5.2710
CB7	373.45	82.69	290.76	323.65	0.8984	5.3902
					MEAN	5.0728

11/28/2012

Bucket	Full Mass (g)	Bucket Tare Mass (g)	Water Mass (g)	Catchment Area (cm²)	10 min Rainfall Rate (cm hour⁻¹)	1 hour Rainfall Rate (cm hour⁻¹)
CB1	272.91	83.87	189.04	323.65	0.5841	5.8408
CB2	231.17	83.01	148.16	323.65	0.4578	4.5777
CB3	251.68	83.89	167.79	323.65	0.5184	5.1842
CB4	249.9	84.00	165.9	323.65	0.5126	5.1258
CB5	240.92	85.95	154.97	323.65	0.4788	4.7881
CB6	264.49	83.14	181.35	323.65	0.5603	5.6032
CB7	233.56	82.69	150.87	323.65	0.4661	4.6614
					MEAN	5.1116

11/28/2012

Bucket	Full Mass (g)	Bucket Tare Mass (g)	Water Mass (g)	Catchment Area (cm²)	10 min Rainfall Rate (cm hour⁻¹)	1 hour Rainfall Rate (cm hour⁻¹)
CB1	254.88	83.87	171.01	323.65	0.5284	5.2837
CB2	248.51	83.01	165.5	323.65	0.5113	5.1135
CB3	268.1	83.89	184.21	323.65	0.5692	5.6916
CB4	249.12	84.00	165.12	323.65	0.5102	5.1017
CB5	238.89	85.95	152.94	323.65	0.4725	4.7254
CB6	234.21	83.14	151.07	323.65	0.4668	4.6676
CB7	236.29	82.69	153.6	323.65	0.4746	4.7458
					MEAN	5.0470

11/29/2012

Bucket	Full Mass (g)	Bucket Tare Mass (g)	Water Mass (g)	Catchment Area (cm²)	10 min Rainfall Rate (cm hour⁻¹)	1 hour Rainfall Rate (cm hour⁻¹)
CB1	257.61	83.87	173.74	323.65	0.5368	5.3681
CB2	246.3	83.01	163.29	323.65	0.5045	5.0452
CB3	234.41	83.89	150.52	323.65	0.4651	4.6506
CB4	247.44	84.00	163.44	323.65	0.5050	5.0498
CB5	253.47	85.95	167.52	323.65	0.5176	5.1759
CB6	243.7	83.14	160.56	323.65	0.4961	4.9608
CB7	241.32	82.69	158.63	323.65	0.4901	4.9012
					MEAN	5.0217

11/29/2012

Bucket	Full Mass (g)	Bucket Tare Mass (g)	Water Mass (g)	Catchment Area (cm²)	10 min Rainfall Rate (cm hour⁻¹)	1 hour Rainfall Rate (cm hour⁻¹)
CB1	255.25	83.87	171.38	323.65	0.5295	5.2951
CB2	241.49	83.01	158.48	323.65	0.4897	4.8966
CB3	245.63	83.89	161.74	323.65	0.4997	4.9973
CB4	249.38	84.00	165.38	323.65	0.5110	5.1098
CB5	252.65	85.95	166.7	323.65	0.5151	5.1506
CB6	237.05	83.14	153.91	323.65	0.4755	4.7554
CB7	257.93	82.69	175.24	323.65	0.5414	5.4144
					MEAN	5.0884

5/22/2013

Bucket	Full Mass (g)	Bucket Tare Mass (g)	Water Mass (g)	Catchment Area (cm²)	10 min Rainfall Rate (cm hour⁻¹)	1 hour Rainfall Rate (cm hour⁻¹)
CB1	366.41	83.87	282.54	323.65	0.8730	5.2378
CB2	339.59	83.01	256.58	323.65	0.7928	4.7566
CB3	365.35	83.89	281.46	323.65	0.8696	5.2178
CB4	359.81	84.00	275.81	323.65	0.8522	5.1130
CB5	374.29	85.95	288.34	323.65	0.8909	5.3453
CB6	357.88	83.14	274.74	323.65	0.8489	5.0932
CB7	343.92	82.69	261.23	323.65	0.8071	4.8428
					MEAN	5.0866

5/23/2013

Bucket	Full Mass (g)	Bucket Tare Mass (g)	Water Mass (g)	Catchment Area (cm²)	10 min Rainfall Rate (cm hour⁻¹)	1 hour Rainfall Rate (cm hour⁻¹)
CB1	261.59	83.87	177.72	323.65	0.5491	5.4910
CB2	258.19	83.01	175.18	323.65	0.5413	5.4126
CB3	282.3	83.89	198.41	323.65	0.6130	6.1303
CB4	234.91	84.00	150.91	323.65	0.4663	4.6627
CB5	212.49	85.95	126.54	323.65	0.3910	3.9097
CB6	257.41	83.14	174.27	323.65	0.5384	5.3844
CB7	217.27	82.69	134.58	323.65	0.4158	4.1581
					MEAN	5.0213

5/23/2013

Bucket	Full Mass (g)	Bucket Tare Mass (g)	Water Mass (g)	Catchment Area (cm²)	10 min Rainfall Rate (cm hour⁻¹)	1 hour Rainfall Rate (cm hour⁻¹)
CB1	271.48	83.87	187.61	323.65	0.5797	5.7966
CB2	267.33	83.01	184.32	323.65	0.5695	5.6950
CB3	249.11	83.89	165.22	323.65	0.5105	5.1048
CB4	257.38	84.00	173.38	323.65	0.5357	5.3569
CB5	235.61	85.95	149.66	323.65	0.4624	4.6241
CB6	232.85	83.14	149.71	323.65	0.4626	4.6256
CB7	223.47	82.69	140.78	323.65	0.4350	4.3497
					MEAN	5.0790

5/29/2013

Bucket	Full Mass (g)	Bucket Tare Mass (g)	Water Mass (g)	Catchment Area (cm²)	10 min Rainfall Rate (cm hour⁻¹)	1 hour Rainfall Rate (cm hour⁻¹)
CB1	248.95	83.87	165.08	323.65	0.5100	5.1005
CB2	261.9	83.01	178.89	323.65	0.5527	5.5272
CB3	231.11	83.89	147.22	323.65	0.4549	4.5487
CB4	268.75	84.00	184.75	323.65	0.5708	5.7082
CB5	250.15	85.95	164.2	323.65	0.5073	5.0733
CB6	254.81	83.14	171.67	323.65	0.5304	5.3041
CB7	228.24	82.69	145.55	323.65	0.4497	4.4971
					MEAN	5.1084

5/29/2013

Bucket	Full Mass (g)	Bucket Tare Mass (g)	Water Mass (g)	Catchment Area (cm²)	10 min Rainfall Rate (cm hour⁻¹)	1 hour Rainfall Rate (cm hour⁻¹)
CB1	252.59	83.87	168.72	323.65	0.5213	5.2130
CB2	271.21	83.01	188.2	323.65	0.5815	5.8148
CB3	243.5	83.89	159.61	323.65	0.4931	4.9315
CB4	238.41	84.00	154.41	323.65	0.4771	4.7708
CB5	240.24	85.95	154.29	323.65	0.4767	4.7671
CB6	247.47	83.14	164.33	323.65	0.5077	5.0773
CB7	244.66	82.69	161.97	323.65	0.5004	5.0044
					MEAN	5.0827

APPENDIX C. CONCENTRATION OF METALS IN GRASS TISSUE AT ONE AND SIX MONTHS FOLLOWING VEGETATION WITH TALL FESCUE.

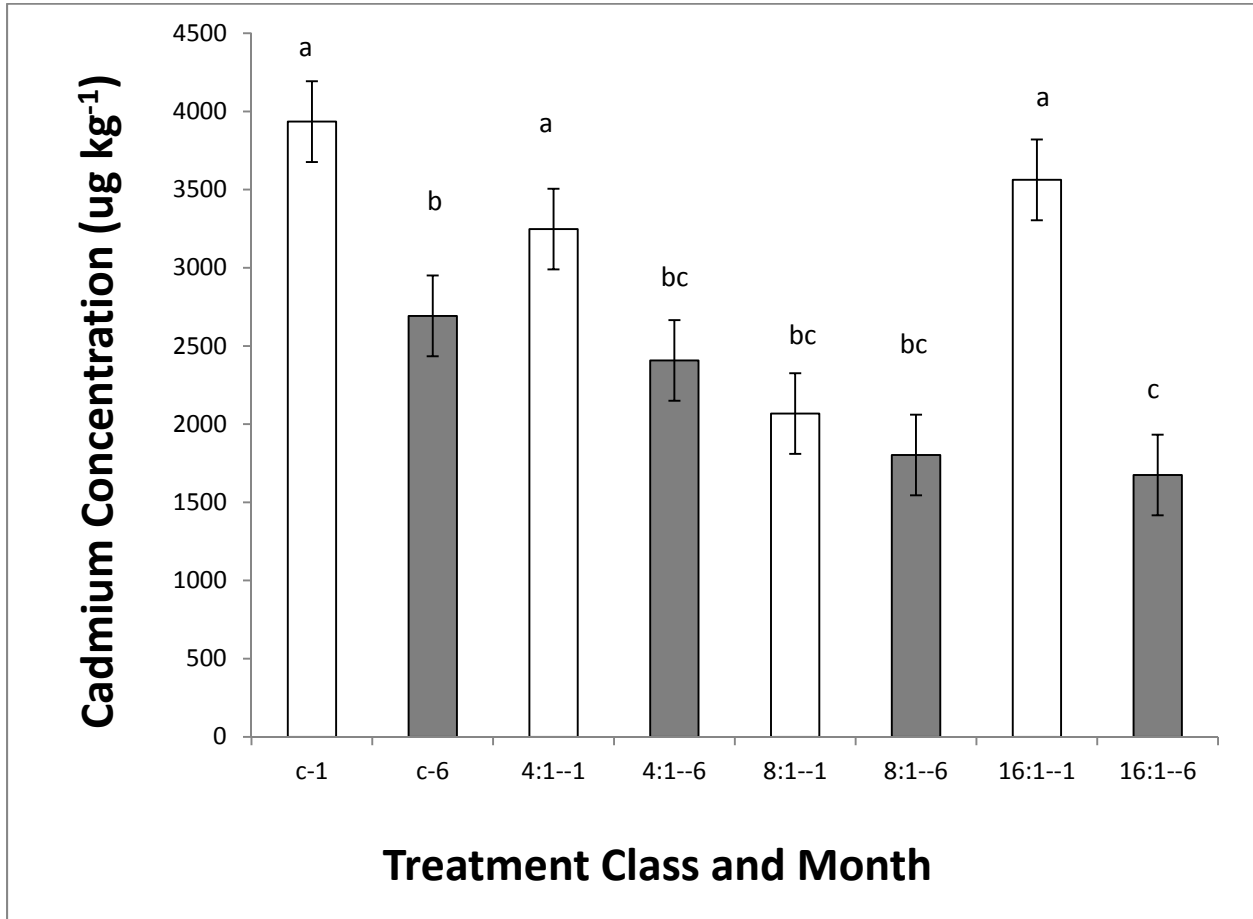


Figure C.1. Arithmetic mean of cadmium concentrations of above ground grass tissue one (1) and six (6) months after vegetation with tall fescue (*Festuca arundinacea*). Error bars represent standard error.

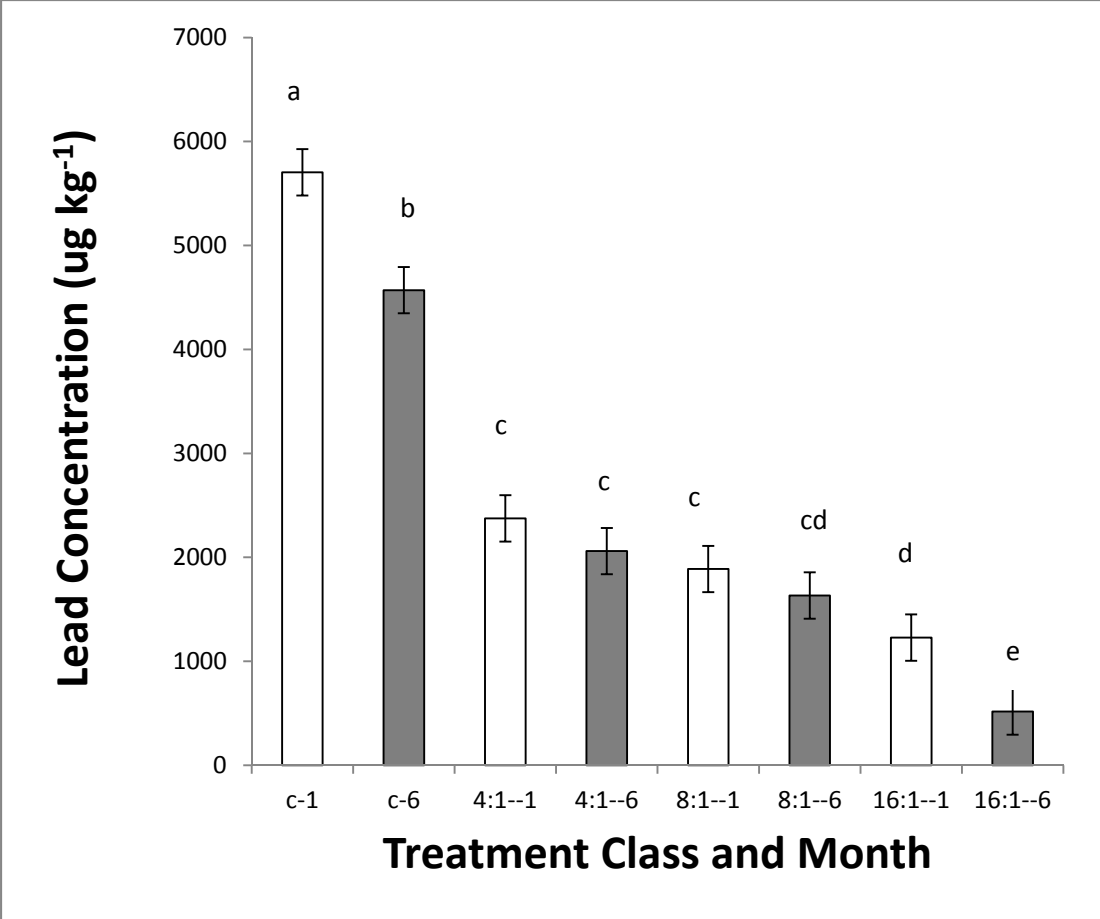


Figure C.2. Arithmetic mean of lead concentrations of above ground grass tissue one (1) and six (6) months after vegetation with tall fescue (*Festuca arundinacea*). Error bars represent standard error.

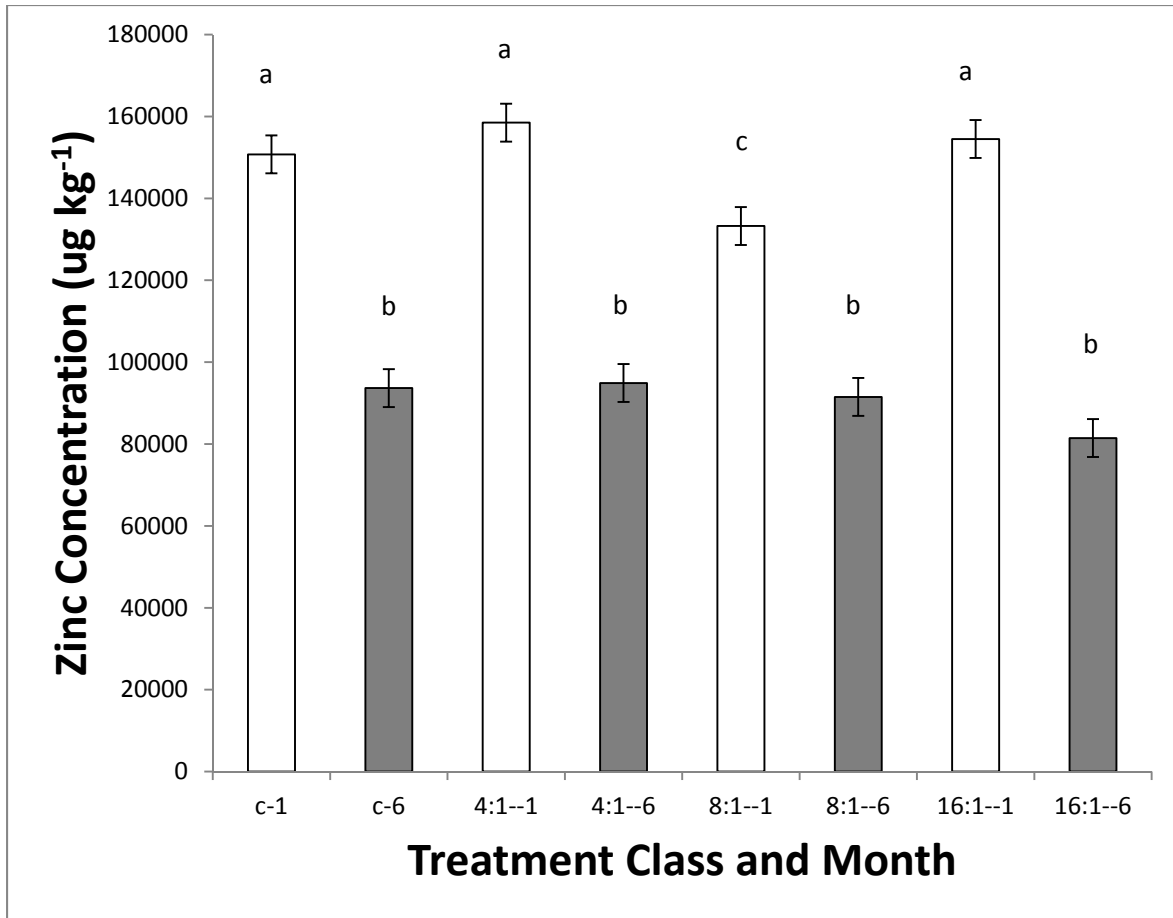


Figure C.3. Arithmetic mean of zinc concentrations of above ground grass tissue one (1) and six (6) months after vegetation with tall fescue (*Festuca arundinacea*). Error bars represent standard error.

APPENDIX D. SOIL AND WATER CHEMISTRY RESULTS FROM AMENDED AND UN-AMENDED SOILS.

Table D.1. Soil pH in water and in 0.01M CaCl₂ at listed days after first P treatment. Values represent the arithmetic mean of four repetitions per treatment level.

Treatment class	Days after treatment	pH in water	pH in 0.02M CaCl ₂
Control	30	7.98	7.70
2:1 P:Pb		7.56	7.38
4:1 P:Pb		7.28	7.04
8:1 P:Pb		7.12	6.91
Control	60	7.88	7.65
4:1 P:Pb		6.90	6.51
8:1 P:Pb		6.09	5.80
16:1 P:Pb		5.43	5.54
Control	90	7.91	7.80
4:1 P:Pb		6.99	6.69
8:1 P:Pb		6.34	6.02
16:1 P:Pb		5.78	5.61
Control	180	7.95	7.73
4:1 P:Pb		7.34	7.11
8:1 P:Pb		7.03	6.57
16:1 P:Pb		6.84	6.29
Control	270	7.90	7.68
4:1 P:Pb		7.10	6.68
8:1 P:Pb		7.80	7.57
16:1 P:Pb		7.03	6.90
Control	450	8.02	7.92
4:1 P:Pb		7.40	7.44
8:1 P:Pb		8.11	7.81
16:1 P:Pb		7.43	7.34

Table D.2. Arithmetic mean results of water chemistry analytes from the first (un-vegetated) rainfall simulation.

Treatment Class	Total Phosphorus (mg L ⁻¹)	Diss. Orthophosphates (mg L ⁻¹)	Diss. Cadmium (µg L ⁻¹)	Diss. Lead (µg L ⁻¹)	Diss. Zinc (µg L ⁻¹)	Total Cadmium (µg L ⁻¹)	Total Lead (µg L ⁻¹)	Total Zinc (µg L ⁻¹)
Control	1.03 (±0.02) †	0.03 (±0.01)	0.17 (±0.03)	9.15 (±0.7)	8.67(±0.7)	34.93 (±5.5)	8657(±278)	1797 (±342)
4:1	4.53 (±0.41)	0.93(±0.03)	0.16 (±0.00)	8.79(±0.43)	9.14(±0.17)	45.75(±6.1)	10802 (±476)	2905(±543)
8:1	9.70 (±0.62)	1.63 (±0.05)	0.11(±0.00)	8.31 (±0.42)	6.93 (±0.11)	72.45 (±11.7)	15325 (±205)	4352 (±601)
16:1	36.15 (±4.51)	4.05(±0.21)	0.17 (±0.00)	9.25 (±0.39)	6.16 (±0.21)	78.70 (±11.1)	14750 (±177)	4555 (±618)

† Error in parentheses represent standard error.

Table D.3. Arithmetic mean results of water chemistry analytes from the second (vegetated) rainfall simulation.

Treatment Class	Total Phosphorus (mg L ⁻¹)	Diss. Orthophosphates (mg L ⁻¹)	Diss. Cadmium (μg L ⁻¹)	Diss. Lead (μg L ⁻¹)	Diss. Zinc (μg L ⁻¹)	Total Cadmium (μg L ⁻¹)	Total Lead (μg L ⁻¹)	Total Zinc (μg L ⁻¹)
Control	0.54 (±0.07) †	0.31 (±0.07)	0.42 (±0.05)	5.25 (±2.15)	23.58 (±3.95)	0.86 (±0.11)	21.88 (±5.04)	43.75 (±5.39)
4:1	0.91 (±0.03)	0.63(±0.04)	0.23 (±0.02)	2.58 (±1.03)	24.28 (±3.13)	0.73 (±0.08)	21.33 (4.23)	56.73 (±8.95)
8:1	1.33 (±0.16)	0.76 (±0.09)	0.24 (±0.05)	5.49 (±1.30)	23.25 (±5.43)	0.69 (±0.05)	35.98 (±2.27)	66.85 (±3.71)
16:1	2.07 (±0.13)	1.67 (±0.18)	0.34 (±0.06)	3.13 (±1.32)	34.63(±6.85)	0.95 (±0.06)	28.20 (±6.29)	71.03 (±14.74)

† Error in parentheses represent standard error.

Table D.4. Water, sediment, and mass lost results from the first and second rainfall simulation events.

Rainfall Simulation and Treatment Class	Mass Total (soil + sediment)	Sediment	Mass Water Only	Sediment Volume	Total Volume	Total P	Total Cd	Total Pb	Total Zn	Runoff Area	P loss	Cd loss	Pb loss	Zn loss
	g	g	g	cm ³	L	mg L ⁻¹	µg L ⁻¹	µg L ⁻¹	µg L ⁻¹	m ²	mg/m ²	mg/m ²	mg/m ²	mg/m ²
RFS1-Control	2672.2	13.43	2658.8	5.07	2.66	1.03	34.93	8657	1797	0.15	18.29	0.620	153.738	31.913
RFS1-4:1	2513.8	11.17	2502.6	4.22	2.51	4.53	45.75	10802	2905	0.15	75.71	0.765	180.527	48.549
RFS1-8:1	2711.3	15.81	2695.5	5.97	2.70	9.7	72.45	15325	4352	0.15	174.69	1.305	275.997	78.378
RFS1-16:1	2505.2	16.32	2488.9	6.16	2.50	36.15	78.7	14750	4555	0.15	601.31	1.309	245.348	75.767
RFS2-Control	2615.9	0.66	2615.3	0.25†	2.62	0.54	0.86	21.88	43.75	0.15	9.42	0.015	0.382	0.763
RFS2-4:1	2762.3	0.57	2761.7	0.22†	2.76	0.91	0.73	21.33	56.73	0.15	16.76	0.013	0.393	1.045
RFS2-8:1	2775.2	0.88	2774.3	0.33†	2.77	1.33	0.69	35.98	66.85	0.15	24.60	0.013	0.666	1.237
RFS2:16:1	2750.6	0.67	2749.9	0.25†	2.75	2.07	0.95	28.2	71.03	0.15	37.95	0.017	0.517	1.302

†Mass recovered was insufficient for analysis via Mehlich 3 for phosphorus.

Table D.5. Effect of rainfall simulation and treatment class on phosphorus loss from test beds.

Simulation and Treatment Class	Simulation and Treatment Class							
	RFS1-Control	RFS1-4:1	RFS1-8:1	RFS1-16:1	RFS2-Control	RFS2-4:1	RFS2-8:1	RFS2:16:1
RFS1-Control	n/a	0.926	0.007	p<0.001	0.784	0.893	0.832	0.841
RFS1-4:1	0.926	n/a	0.259	p<0.001	0.842	0.920	0.947	0.995
RFS1-8:1	0.007	0.259	n/a	p<0.001	0.004	0.006	0.008	0.020
RFS1-16:1	p<0.001	p<0.001	p<0.001	n/a	p<0.001	p<0.001	p<0.001	p<0.001
RFS2-Control	0.784	0.842	0.004	p<0.001	n/a	0.469	0.399	0.887
RFS2-4:1	0.893	0.920	0.006	p<0.001	0.469	n/a	0.710	0.688
RFS2-8:1	0.832	0.947	0.008	p<0.001	0.399	0.710	n/a	0.468
RFS2:16:1	0.841	0.995	0.020	p<0.001	0.887	0.688	0.468	n/a

Statistically significant effects (p-values <0.05) are noted in bold.

Table D.6. Effect of rainfall simulation and treatment class on total cadmium loss from test beds.

Simulation and Treatment Class								
Simulation and Treatment Class	p-values							
	RFS1-Control	RFS1-4:1	RFS1-8:1	RFS1-16:1	RFS2-Control	RFS2-4:1	RFS2-8:1	RFS2:16:1
RFS1-Control	n/a	0.968	0.006	0.007	0.023	0.024	0.025	0.021
RFS1-4:1	0.968	n/a	0.040	0.037	0.004	0.003	0.003	0.005
RFS1-8:1	0.006	0.040	n/a	0.908	p<0.001	p<0.001	p<0.001	p<0.001
RFS1-16:1	0.007	0.037	0.908	n/a	p<0.001	p<0.001	p<0.001	p<0.001
RFS2-Control	0.023	0.004	p<0.001	p<0.001	n/a	0.954	0.997	0.788
RFS2-4:1	0.024	0.003	p<0.001	p<0.001	0.954	n/a	0.981	0.898
RFS2-8:1	0.025	0.003	p<0.001	p<0.001	0.997	0.981	n/a	0.790
RFS2:16:1	0.021	0.005	p<0.001	p<0.001	0.788	0.898	0.790	n/a

Statistically significant effects (p-values <0.05) are noted in bold.

Table D.7. Effect of rainfall simulation and treatment class on total lead loss from test beds.

Simulation and Treatment Class								
Simulation and Treatment Class	p-values							
	RFS1-Control	RFS1-4:1	RFS1-8:1	RFS1-16:1	RFS2-Control	RFS2-4:1	RFS2-8:1	RFS2:16:1
RFS1-Control	n/a	0.890	0.577	0.012	p<0.001	p<0.001	p<0.001	p<0.001
RFS1-4:1	0.890	n/a	0.998	0.176	p<0.001	p<0.001	p<0.001	p<0.001
RFS1-8:1	0.577	0.998	n/a	0.448	p<0.001	p<0.001	p<0.001	p<0.001
RFS1-16:1	0.012	0.176	0.448	n/a	p<0.001	p<0.001	p<0.001	p<0.001
RFS2-Control	p<0.001	p<0.001	p<0.001	p<0.001	n/a	0.885	0.898	0.732
RFS2-4:1	p<0.001	p<0.001	p<0.001	p<0.001	0.885	n/a	0.976	0.883
RFS2-8:1	p<0.001	p<0.001	p<0.001	p<0.001	0.898	0.976	n/a	0.741
RFS2:16:1	p<0.001	p<0.001	p<0.001	p<0.001	0.732	0.883	0.741	n/a

Statistically significant effects (p-values <0.05) are noted in bold.

Table D.8. Effect of rainfall simulation and treatment class on total zinc loss from test beds.

Simulation and Treatment Class	Simulation and Treatment Class							
	p-values							
	RFS1-Control	RFS1-4:1	RFS1-8:1	RFS1-16:1	RFS2-Control	RFS2-4:1	RFS2-8:1	RFS2:16:1
RFS1-Control	n/a	0.476	p<0.001	0.002	0.048	0.048	0.049	0.049
RFS1-4:1	0.476	n/a	0.049	0.086	p<0.001	p<0.001	p<0.001	p<0.001
RFS1-8:1	p<0.001	0.049	n/a	0.854	p<0.001	p<0.001	p<0.001	p<0.001
RFS1-16:1	0.002	0.086	0.854	n/a	p<0.001	p<0.001	p<0.001	p<0.001
RFS2-Control	0.048	p<0.001	p<0.001	p<0.001	n/a	0.974	0.589	0.631
RFS2-4:1	0.048	p<0.001	p<0.001	p<0.001	0.974	n/a	0.884	0.711
RFS2-8:1	0.049	p<0.001	p<0.001	p<0.001	0.589	0.884	n/a	0.972
RFS2:16:1	0.049	p<0.001	p<0.001	p<0.001	0.631	0.711	0.972	n/a

Statistically significant effects (p-values <0.05) are noted in bold.

APPENDIX E. ADDITIONAL SPECTRA FROM X-RAY ABSORPTION NEAR EDGE SPECTROSCOPY ANALYSIS

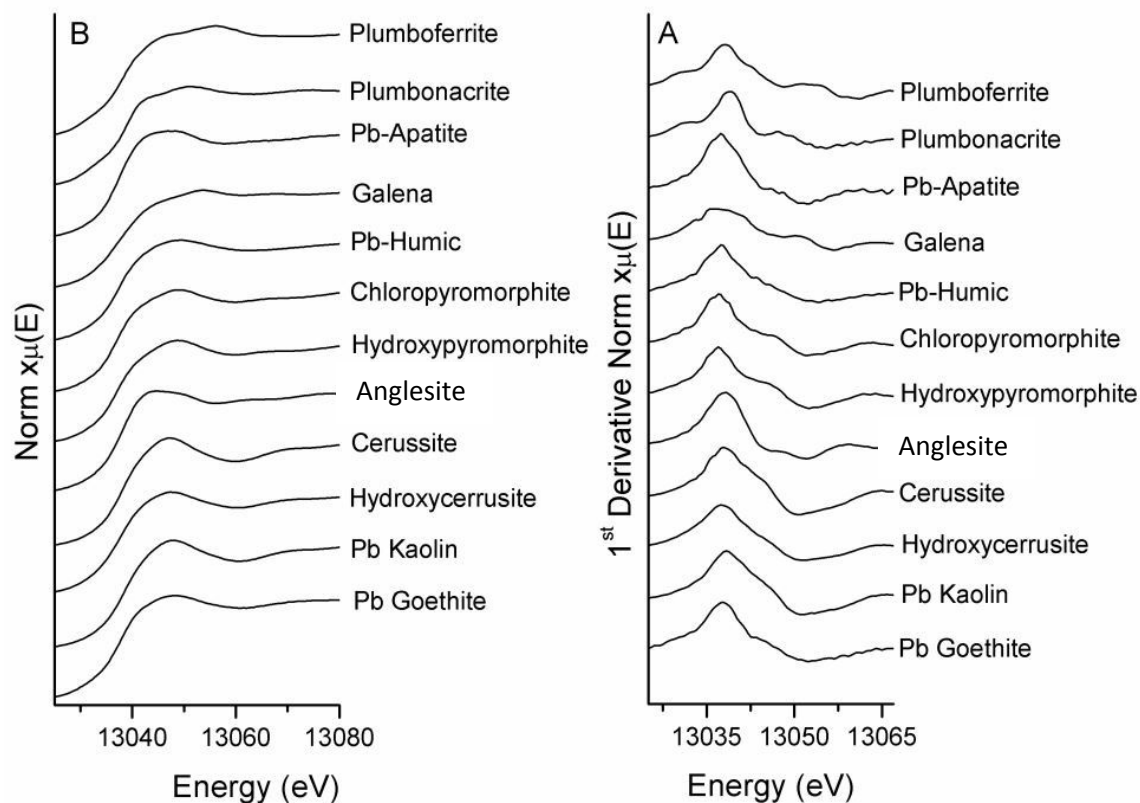


Figure E.1. Normalized and first derivative of normalized x-ray absorption near edge spectroscopy (XANES) spectra of reference samples employed as model components for linear combination fitting.

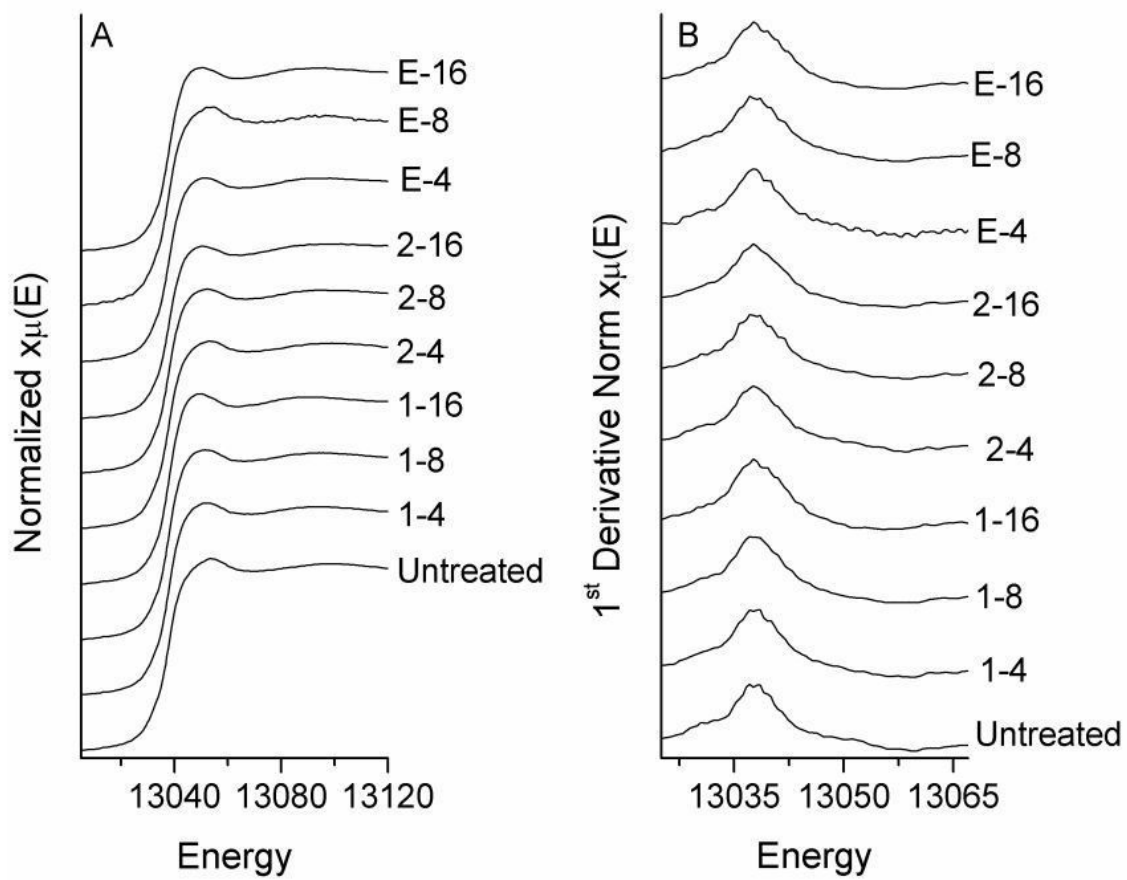


Figure E.2. Normalized and first derivative of normalized x-ray absorption near edge spectroscopy (XANES) spectra of untreated soils and select treated soils.